Published in "Journal of Vertebrate Paleontology 34(2): 327–352, 2014"
which should be cited to refer to this work.

OSTEOLOGY, RELATIONSHIPS, AND ECOLOGY OF *ANNEMYS* (TESTUDINES, EUCRYPTODIRA) FROM THE LATE JURASSIC OF SHAR TEG, MONGOLIA, AND PHYLOGENETIC DEFINITIONS FOR XINJIANGCHELYIDAE, SINEMYDIDAE, AND MACROBAENIDAE

MÁRTON RABI,[*,1,2,3] VLADIMIR B. SUKHANOV,[4] VERA N. EGOROVA,[4] IGOR DANILOV,[5] and WALTER G. JOYCE[1,6]
[1]Institut für Geowissenschaften, University of Tübingen, Hölderlinstraße 12, 72074 Tübingen, Germany, iszkenderun@gmail.com;
[2]Department of Paleontology, Eötvös Loránd University, Pázmány Péter sétány 1/C, 1117 Budapest, Hungary;
[3]MTA–ELTE Lendület Dinosaur Research Group, Budapest, Hungary;
[4]Paleontological Institute of the Russian Academy of Sciences, Profsoyuznaya Str. 123, Moscow, 117997, Russia;
[5]Zoological Institute of the Russian Academy of Sciences, Universitetskaya Emb. 1, 199034 Saint Petersburg, Russia;
[6]Institute for Geosciences, University of Fribourg, Chemin du Musée 6, 1700 Fribourg, Switzerland

ABSTRACT—A complete description of the xinjiangchelyid turtles *Annemys levensis* and *A. latiens* is provided, based on all available material from the Upper Jurassic type locality of Shar Teg, Mongolia. *Annemys latiens* was previously known almost exclusively from shell material, but an undescribed skull from Shar Teg is referable to this species and its distinct morphology confirms the presence of two taxa at this locality. *Annemys latiens* has an elongated skull that markedly differs in proportions from those of *A. levensis* and resembles the shape of some recent, piscivorous turtles. The overall similarity of the shells of the two *Annemys* species combined with significant differences in the skull indicate that these turtles probably partitioned the aquatic niche by exploring different feeding strategies. Among xinjiangchelyids, at least three different skull morphotypes can be differentiated, which implies a moderate level of ecological diversification among Late Jurassic Asian turtles. Phylogenetic analysis weakly supports the inclusion of *Annemys* spp. into Xinjiangchelyidae and places xinjiangchelyids at the stem of Testudines, but the latter result is considered tentative. Phylogenetic definitions of Xinjiangchelyidae, Sinemydidae, and Macrobaenidae are provided for nomenclatural clarity and precision.

SUPPLEMENTAL DATA—Supplemental materials are available for this article

INTRODUCTION

The fossil turtles *Annemys latiens* Sukhanov and Narmandakh, 2006, and *Annemys levensis* Sukhanov and Narmandakh, 2006, are represented by several well-preserved specimens from the Upper Jurassic locality of Shar Teg, Mongolia, and are among the most important representatives of the early eucryptodiran radiation (Sukhanov, 2000; Danilov and Parham, 2006, 2008; Rabi et al., 2010). In particular, *A. levensis* is one of the most complete and best-preserved Jurassic turtles known worldwide and therefore represents a key taxon in our understanding of the early evolution of Asian eucryptodires.

Abundant remains of *Annemys* were collected from Shar Teg by the Joint Soviet-Mongolian Paleontological Expedition during the field seasons of 1984, 1987, and 1989 and a Mongolian team led by R. Barsbold in 1985. Sukhanov (2000) provided an initial description and reconstructions of the more complete cranial and shell material, but only used the names *A. levensis* and *A. latiens* to informally refer to the two species that he recognized. These names therefore remained unavailable according to the rules of the International Commission on Zoological Nomenclature (ICZN; 1999). In a subsequent paper, Sukhanov and Narmandakh (2006) formally named and diagnosed *A. levensis* and *A. latiens,* provided a photograph of the holotype shell of *A. levensis*, but otherwise referred to the preliminary description of Sukhanov (2000). Previously, *A. latiens* had been known only from shells and undescribed skull fragments, but we here demonstrate that a fairly complete skull can be also referred to this species. The vast majority of fragmentary shell, girdle, and appendicular material, by contrast, are referable to *Annemys* sp. only. In spite of the importance of these taxa, a detailed description is still lacking. With this contribution, we intend to rectify this situation by describing and illustrating in detail the bulk of the *A. latiens* and *A. levensis* material from Shar Teg.

Previous phylogenetic studies (i.e., Anquetin, 2012; Tong et al., 2012b) that incorporated *A. levensis* utilized the available literature (Sukhanov, 2000; Sukhanov and Narmandakh, 2006) when scoring this taxon. The resulting phylogenies are in conflict with each another, in part likely because this taxon received different character scorings. Our detailed description of this taxon provides an opportunity to rigorously test the phylogenetic position of this important taxon within a global, cladistic context based on all available material and may therefore provide a more accurate phylogenetic hypothesis.

The description of phylogenetic results within Eucryptodira has been greatly hampered by a nomenclatural system that is universally agreed to be confusing. The suprageneric names Sinemydidae Ye, 1963, Macrobaenidae Sukhanov, 1964, and Xinjiangchelyidae Nessov in Kaznyshkin, Nalbandyan, and Nessov, 1990, were introduced by taxonomists to group various fossil eucryptodires. However, given that most characters that were used to diagnose these groups have since been shown to represent plesiomorphies (e.g., Sukhanov, 2000; Rabi et al., 2010) and given that changing phylogenies have not allowed some well-diagnosed clades worth naming to be identified (e.g., Gaffney and Ye, 1992; Gaffney, 1996; Brinkman and Wu, 1999; Parham

*Corresponding author.
Color versions of one or more of the figures in the article can be found online at www.tandfonline.com/ujvp.

and Hutchison, 2003; Gaffney et al., 2007; Joyce, 2007; Anquetin, 2012; Tong et al., 2012a, 2012b), most authors have resorted to placing these names in quotation marks to indicate their likely paraphyly while tolerating the resulting taxonomic imprecision. We herein attempt to resolve this situation by providing phylogenetic definitions of these names and to thereby stabilize their taxonomic meanings. Sinemydidae, Macrobaenidae, and Xinjiangchelyidae refer to monophyletic clades throughout this contribution (see Phylogenetic Definitions below) and are therefore not placed in quotation marks. Finally, in light of new data on the skull morphology of *Annemys*, we discuss the ecological diversity of xinjiangchelyids during the Late Jurassic.

Institutional Abbreviation—**PIN**, Paleontological Institute of the Russian Academy of Sciences, Moscow.

Nomenclature—The nomenclature of the skull used herein follows Gaffney (1972), that of the shell follows Hutchison and Bramble (1981). All higher taxonomic names are clade names as defined by Joyce et al. (2004) or in the section Phylogenetic Definitions.

GEOLOGIC SETTINGS

The material of *Annemys levensis*, *A. latiens*, and *A.* sp. described herein all originates from the locality of Shar Teg, which is situated in the Transaltai Gobi, approximately 100 km east-southeast of the town of Altai, within Altai Somon District in the southern part of Govi Altai Aimag Province, Mongolia. The locality is surrounded by the Az Bogdo, the Edrengiin Nuru, and the Atas Bogdo mountains from the north, northeast, and south, respectively. The Shar Teg locality spreads across several mesas and was named after one of these, Shar Teg, after it was discovered by V. Yu. Reshetov of the Joint Soviet-Mongolian Expedition in 1984 (Gubin and Sinitza, 1996). The type specimen of *Annemys levensis*, including other material of *Annemys*, were discovered in the same year, approximately halfway between the Shar Teg and Ulan Malgait hills, and 4–5 km west of the former.

The expeditions of 1987 and 1989 led by Y. M. Gubin worked on the stratigraphy of Shar Teg and recognized two units separated by a distinct limestone-caliche horizon. The lower Shar Teg beds are more widely distributed in the southwestern part of the locality, whereas the overlaying Ulan Malgait beds are more common in the northeastern part. Both beds are present along the Ulan Malgait and the Shar Teg hills. The *Annemys latiens, A. levensis*, and indeterminate *Annemys* material described herein originate from the Ulan Malgait beds. A Mongolian team collected the type material of *A. latiens* in 1985 and the remaining specimens described herein were collected in 1989. All *A. latiens* material, however, lacks more precise stratigraphic and locality data. In 2002, a joint Japanese-Mongolian Expedition collected a shell with articulated neck and skull in sandstones in the lower part of the Ulan Malgait beds (Watabe et al., 2004:pl. 4, fig. 6), but this specimen was not available to us and was therefore not included in our study.

The Ulan Malgait beds form a mostly siliciclastic unit composed of red, gray, brown, or yellow siltstones with interbedded coarse and fine sandstones. The turtle remains were found in four different sandstone horizons together with gastropods, bivalves, fishes, crocodilians, and sauropod dinosaurs (Gubin and Sinitza, 1996; Watabe et al., 2004).

The 'Shar Teg' beds are characterized by the alternation of sandstones with red, yellow, gray, brown, and green siltstones with limestone interbeddings in the lower part. A single layer of gray argillites and clays yielded a notably different vertebrate fauna relative to the Ulan Malgait beds, including the turtle *Shartegemys laticentralis* Sukhanov and Narmandakh, 2006, and isolated elements of insects, fishes, brachyopoid temnospondyls, theropod dinosaurs, tritylodontid cynodonts, and mammals (Gubin and Sinitza, 1996; Watabe et al., 2004).

The depositional environment of the Shar Teg beds is interpreted as a 20–40-km-long lake that episodically dried up during arid phases with a gradual transition from lacustrine to fluvial sedimentation. Conversely, the Ulan Malgait beds are considered to represent an extensive fluvial system and the vertebrate-bearing sandstone lenses are interpreted as crevasse splay (flood) deposits (Gubin and Sinitza, 1996; Watabe et al., 2004).

The ages of the Shar Teg and Ulan Malgait beds are poorly resolved. Biostratigraphic data based on stoneflies from the Shar Teg beds indicate a Middle Jurassic age, whereas a more recent study of mayflies argued for a Late Jurassic age (Sinitshenkova, 1995, 2002). No biostratigraphic data are available from the overlying Ulan Malgait beds (Watabe et al., 2004).

SYSTEMATIC PALEONTOLOGY

TESTUDINATA Klein, 1760
TESTUDINES Batsch, 1788
PANCRYPTODIRA Joyce, Parham, and Gauthier, 2004
XINJIANGCHELYIDAE Nessov in Kaznyshkin, Nalbandyan, and Nessov, 1990
ANNEMYS Sukhanov and Narmandakh, 2006

Types Species—*Annemys latiens* Sukhanov and Narmandakh, 2006.

Included Species—*Annemys levensis* Sukhanov and Narmandakh, 2006.

Distribution—Late Jurassic of Shar Teg locality, Govi Altai Aimag, Mongolia (Sukhanov, 2000; Sukhanov and Narmandakh, 2006) and late Middle Jurassic to early Late Jurassic of Wucaiwan area, Junggar Basin, Xinjiang Autonomous Uyghur Province, China (Brinkman et al., 2013).

Diagnosis—See Sukhanov and Narmandakh (2006) for a non-differential diagnosis. The skull of *Annemys* differs from *Xinjiangchelys radiplicatoides* Brinkman, Eberth, Clark, Xing, and Wu, 2013, in being flattened, having a deeper upper temporal emargination, a longer supraoccipital crest, and reduced basioccipital tubera; from *Hangaiemys* (*Kirgizemys*) *hoburensis* Sukhanov and Narmandakh, 1974, and *Kirgizemys dmitrievi* Nessov and Khosatzky, 1981, in the presence of a laterally widely open foramen jugulare posterius, and the absence of paired pits on the basisphenoid. The latter also differentiates *Annemys* from Shar Teg from *Sinemys* spp. (sensu Brinkman and Peng, 1993a), *Dracochelys bicuspis* Gaffney and Ye, 1992, and *Ordosemys* spp. (sensu Danilov and Parham, 2007, and Tong et al., 2004). The shell of *Annemys* differs from *Xinjiangchelys* spp. (sensu Brinkman et al., 2008, and Brinkman et al., 2013) in the vertebrals 2 and 3 being almost as long as wide, vertebral 4 being wider than vertebrals 2 and 3, the placement of the vertebral 3/4 sulcus on neural 6, and an interrupted neural row that allows a midline contact between costal 7s; differs from *Shartegemys laticentralis* in the square epiplastra; differs from *Chengyuchelys* spp. (sensu Tong et al., 2012b), *Protoxinjiangchelys salis* Tong, Danilov, Ye, Ouyang, and Peng, 2012a, and *Yanduchelys delicatus* Peng, Ye, Gao, Shu, and Jiang, 2005 (sensu Tong et al., 2012b) in the presence of a ligamentous carapace-plastron attachment; further differs from *Chengyuchelys* spp. in the vertebral 5 not overlapping onto peripheral 10; differs from *Tienfuchelys* spp. (sensu Tong et al., 2012b) in having four pairs of inframarginals; and differs from *Hangaiemys* (*Kirgizemys*) *hoburensis*, *Sinemys lens* Wiman, 1930, and *Ordosemys* spp. in the relatively shorter dorsal rib 1, extension of marginals 4–8 onto costals, square-shaped epiplastron that is tightly sutured to the ento- and hyoplastron, reduced epiplastral process present, extragulars present, femoro-anal sulcus omega-shaped and extending onto hypoplastron, and sinuous midline sulcus.

ANNEMYS LEVENSIS Sukhanov and Narmandakh, 2006
(Figs. 1–5)

Annemys levensis Sukhanov and Narmandakh, in press, in Sukhanov, 2000:314, fig. 17.2 (unavailable under articles 13.1.1 and 16.1 of the International Commission on Zoological Nomenclature [1999]).

Annemys levensis Sukhanov and Narmandakh, 2006:120, fig. 1a, b (original description).

Xinjiangchelys levensis (Sukhanov and Narmandakh, 2006), Tong et al., 2012b:107 (new combination).

Holotype—PIN 4636-4, associated skull and mandible (PIN 4636-4-2), shell, right femur, right humerus, right scapula and fragment of coracoid, and incomplete right pelvic girdle (PIN 4636-4-1).

Locality and Horizon—Shar Teg locality, Govi Altai Aimag, Mongolia, Upper Jurassic, Ulan Malgait beds.

Revised Diagnosis—A species of *Annemys* differing from *A. latiens* in the presence of a broader and shorter skull, partially separated prefrontals, more extensive contributions of the frontal and the jugal to the orbital rim, quadrangular neural 1, longer and narrower posterior plastral lobe, and relatively narrower anterior projection of the anal scales.

ANNEMYS LATIENS Sukhanov and Narmandakh, 2006
(Figs. 6–10)

Annemys latiens Sukhanov and Narmandakh, in press, in Sukhanov, 2000:317, fig. 17.4 (unavailable under articles 13.1.1 and 16.1 of the International Commission on Zoological Nomenclature [1999]).

Xinjiangchelys latiens (Sukhanov and Narmandakh, in press): Matzke et al., 2004b:1295 (new combination of unavailable name).

Annemys latiens Sukhanov and Narmandakh, 2006:120 (original description).

Xinjiangchelys latiens (Sukhanov and Narmandakh, 2006), Tong et al., 2012b:107 (new combination).

Holotype—PIN 4636-5, an almost complete shell (PIN 4636-5-1), a partial basicranium and lower jaw ramus (PIN 4636-5-2), and other poorly preserved disarticulated cranial elements.

Referred Material—PIN 4636-6-1, an incomplete shell lacking most of the carapace; PIN 4636-6-2, a partial skull associated with PIN 4636-6-1; PIN 4636-7, an almost complete shell and a humerus. All referred material is from the type locality.

Locality and Horizon—Shar Teg locality, Govi Altai Aimag, Mongolia, Upper Jurassic, Ulan Malgait beds.

Revised Diagnosis—A species of *Annemys* differing from *A. levensis* in the presence of a narrower and longer skull, frontals that fully separate the prefrontals, a minor contribution of the frontal and the jugal to the orbital rim, hexagonal neural 1, a shorter and broader posterior plastral lobe, and relatively wider anterior projection of the anal scales.

ANNEMYS SP.
(Figs. 11, 12)

Referred Material—PIN 4636-10, pelvis; PIN 4636-11, scapula; PIN 4636-12, femur; PIN 4636-13, hyoplastron buttress; PIN 4636-14, hypoplastron buttress; PIN 4636-15, peripheral 2; PIN 4636-16, articulated peripheral 6 and peripheral 7; PIN 4636-17, associated peripheral 3; PIN 4636-18, peripheral 5; PIN 4636-19, peripheral 6; PIN 4636-20, peripheral 7; PIN 4636-21, peripheral 8; PIN 4636-22, peripheral 2; PIN 4636-23, peripheral 4.

Remarks—Hundreds of further uncataloged isolated shell and appendicular elements are present in the collection of PIN from Shar Teg. Together with the material listed above, these cannot be identified to the species level and we therefore refer them to *Annemys* sp.

Locality and Horizon—Shar Teg locality, Govi Altai Aimag, Mongolia, Upper Jurassic, Ulan Malgait beds.

PHYLOGENETIC NOMENCLATURE

XINJIANGCHELYIDAE Nessov in Kaznyshkin, Nalbandyan, and Nessov, 1990, converted clade name

Definition—Xinjiangchelyidae refers to the most inclusive clade containing *Xinjiangchelys junggarensis* Ye, 1986, but not *Sinemys lens*, *Macrobaena mongolica* Tatarinov, 1959, or any species of Recent turtle.

Discussion—The name Xinjiangchelyidae was widely used to refer to a poorly defined group of basal eucryptodire taxa from the Jurassic of Asia (see Rabi et al., 2010, for a literature review). Nessov (in Kaznyshkin et al., 1990) originally coined the name along with Xinjiangchelydia, but subsequent workers did not adopt the latter term. Nessov (in Kaznyshkin et al., 1990) provided a diagnosis for Xinjiangchelyidae and synonymized *X. junggarensis* and '*Plesiochelys*' *radiplicatus* Young and Chow, 1953, with the type species of the family, *Xinjiangchelys latimarginalis* (Young and Chow, 1953) (= *Chengyuchelys latimarginalis* sensu Tong et al., 2012b), but it is unclear if he believed this taxon to be more inclusive than *Xinjiangchelys latimarginalis*. Sukhanov (2000) subsequently provided an emended diagnosis for Xinjiangchelyidae and explicitly circumscribed this taxon to include *Xinjiangchelys* spp., *Annemys* from Shar Teg, and the poorly known turtles *Shartegemys laticentralis*, *Undjulemys platensis* Sukhanov and Narmandakh, 2006, and *Tienfuchelys tzuyangensis* Young and Chow, 1953. Although this circumscription was followed by Matzke et al. (2004b), their phylogenetic analysis did not rigorously test the monophyly of the group. Tong et al. (2012a) circumscribed Xinjiangchelyidae as including *X. latimarginalis*, *X. tianshanensis* Nessov, 1995, and *Protoxinjiangchelys salis*, but their phylogenetic analysis revealed this grouping to be paraphyletic relative to the clade formed by *Bashuchelys zigongensis* (Ye, 1982), *Bashuchelys youngi* Tong, Danilov, Ye, Ouyang, and Peng, 2012a, and *Chuannanchelys dashanpuensis* (Fang, 1987). Tong et al. (2012b) circumscribed Xinjiangchelyidae as consisting of *Brodiechelys* spp., *Chengyuchelys* spp., *Protoxinjiangchelys salis*, *Tienfuchelys* spp., *Xinjiangchelys* spp. (including *Annemys* and *Shartegemys* Sukhanov and Narmandakh, 2006), and *Yanduchelys delicatus* Peng, Ye, Gao, Shu, and Jiang, 2005, and provided some support for the monophyly of this group of turtles with a phylogenetic analysis. By contrast, Anquetin (2012) circumscribed Xinjiangchelyidae as consisting of *Xinjiangchelys qiguensis* Matzke, Maisch, Sun, Pfretzschener, and Stöhr, 2004b, *X. latimarginalis* (sensu Peng and Brinkman, 1993), *X. tianshanensis*, *Annemys levensis*, and *Siamochelys peninsularis* Tong, Buffetaut, and Suteethorn, 2002. Various other authors discussed the phylogenetic relationships of *Xinjiangchelys latimarginalis*, but refrained from using the name Xinjiangchelyidae because of the lack of a clear definition for the name (Gaffney et al., 2007; Joyce, 2007; Danilov and Parham, 2008; Sterli, 2010).

Herein, we decided to phylogenetically define the taxon name Xinjiangchelyidae as referring to the most inclusive clade that includes *X. junggarensis*, but no living turtle or the 'essential' members of Sinemydidae or Macrobaenidae (i.e., *Sinemys lens* and *Macrobaena mongolica*). This captures the application of the name as undertaken by Anquetin (2012) and therefore results in the same grouping of turtles for that phylogenetic hypothesis (see above). If this definition is applied to the analysis of Tong et al. (2012a), Xinjiangchelyidae is hypothesized to consist of *X. latimarginalis*, *X. tianshanensis*, *P. salis*, *B. zigongensis*, *B. youngi*, and *C. dashanpuensis*. Our definition of Xinjiangchelyidae cannot be applied to the cladogram of Tong et al. (2012b), because

it includes no extant taxon, *Sinemys lens*, or *Macrobaena mongolica*. In the context of the phylogenetic hypothesis we present herein, *A. levensis*, *X. junggarensis*, and *X. radiplicatoides* are revealed to be part of Xinjiangchelyidae (Fig. 13).

SINEMYDIDAE Ye, 1963, converted clade name

Definition—Sinemydidae refers to the most inclusive clade containing *Sinemys lens* but not *Xinjiangchelys junggarensis, Macrobaena mongolica*, or any species of Recent turtle.

Discussion—The term Sinemydidae has been widely used as a collective name for many Early Cretaceous turtles from Asia (Ye, 1963; Chkhikvadze, 1975, 1977, 1987; Khosatzky and Nessov, 1979; Hutchison and Archibald, 1986; Brinkman and Peng, 1993a, 1993b; Hirayama et al., 2000; Sukhanov, 2000; Brinkman, 2001; Maisch et al., 2003; Matzke et al., 2004a; Tong et al., 2009) and represents another group of questionable utility without an explicit definition (Gaffney, 1996; Gaffney et al., 1998, 2007; Parham and Hutchison, 2003; Joyce, 2007; Danilov and Parham, 2008; Rabi et al., 2010). Sinemydidae was established by Ye (1963) for *Sinemys lens* and *Manchurochelys manchoukuoensis* Endo and Shikama, 1942. Subsequent workers has since proposed a disparate set of circumscriptions for Sinemydidae, including *S. lens*, *Man.* manchoukuoensis*, Macrobaena mongolica, Hangaiemys* (*Kirgizemys*) *hoburensis*, *Kirgizemys exaratus* Nessov and Khosatzky, 1973, and *Yaxartemys longicauda* Ryabinin, 1948 (Chkhikvadze, 1975, 1977, 1987); *Man. manchoukuoensis* and *Sinemys* spp. (Brinkman and Peng, 1993a); *Dracochelys bicuspis*, *Ordosemys* spp., and *Sinemys* spp. (Gaffney, 1996); *Sinemys* spp., *D. bicuspis*, and *H. hoburensis* (Brinkman and Wu, 1999); *D. bicuspis*, *Hongkongochelys yehi* Ye, 1999, *Man. manchoukuoensis*, *Ordosemys* spp., *Sinemys* spp., *Wuguia* spp., and *Yumenemys inflatus* Bohlin, 1953 (Brinkman et al., 2008); and *D. bicuspis*, *Man. manchoukuoensis,* and *Sinemys* spp. (Zhou, 2010a, 2010b), or only *Sinemys* spp. (Sukhanov, 2000; Tong and Brinkman, 2013). Only the circumscriptions of Gaffney (1996) and Zhou (2010a, 2010b) were based on a phylogenetic analysis and therefore unite monophyletic clades.

The summary above amply demonstrates that there is no consensus as to the application of the name Sinemydidae beyond the inclusion of *Sinemys* spp. and the exclusion of extant species of turtles and *Xinjiangchelys junggarensis*. The 'essential' macrobaenid *Macrobaena mongolica* was only included by Chkhikvadze (1975, 1977, 1987). We therefore capture the current consensus by restricting the term Sinemydidae to all turtles more closely related to *S. lens* than to any living turtle or the 'essential' representatives of Xinjiangchelyidae and Macrobaenidae, as already undertaken by Gaffney (1996) and Zhou (2010a, 2010b). If this definition is applied to the topology of Joyce (2007), Sinemydidae is hypothesized to include *S. lens*, *Ordosemys leios* Brinkman and Peng, 1993b, *D. bicuspis*, and *Judithemys sukhanovi* Parham and Hutchison, 2003. According to the topology of Anquetin (2012), this clade consists of *S. lens* and *O. leios*. By contrast, the topologies of Parham and Hutchison (2003), Gaffney et al. (2007), Danilov and Parham (2008), and our proposed phylogeny imply that Sinemydidae only consists of *S. lens*.

MACROBAENIDAE Sukhanov, 1964, converted clade name

Definition—Macrobaenidae refers to the most inclusive clade containing *Macrobaena mongolica* but not *Xinjiangchelys junggarensis*, *Sinemys lens*, or any species of Recent turtle.

Discussion—Macrobaenidae is another name traditionally used for uniting various Asian and North American Cretaceous and Tertiary fossil eucryptodires that are more derived than xinjiangchelyids. Macrobaenidae was established by Sukhanov (1964) for *Mac. mongolica*. Several other taxa were at one or the other time referred to this group, including *Hangaiemys* (*Kirgizemys*) *hoburensis*, *Ordosemys* spp., *Kirgizemys exaratus*, *Asiachelys perforata* Sukhanov and Narmandakh, 2006, and *Anatolemys maximus* Khosatzky and Nessov, 1979 (see Sukhanov, 2000, for a more complete review and references). Some of the listed taxa were variously referred to Sinemydidae by other authors (see above) and the names Sinemydidae and Macrobaenidae therefore often had overlapping circumscription. However, *Xinjiangchelys junggarensis* and *Sinemys lens* were consistently excluded from the group. Interestingly, even though various circumscription of Macrobaenidae are universally agreed to by paraphyletic (e.g., Parham and Hutchison, 2003; Gaffney et al., 2007; Joyce, 2007; Danilov and Parham, 2008; Zhou, 2010b; Sterli and de la Fuente, 2011; Anquetin, 2012), the name giving taxon *Mac. mongolica* was never included in a phylogenetic analysis. There is therefore no precedence of applying the name Macrobaenidae to a monophyletic clade. We decided to restrict the name to the most inclusive clade that includes *Mac. mongolica*, but no living turtle or *X. junggarensis* and *S. lens*. We are not able to apply this name to our cladogram, however, because *Mac. mongolica* is not included as a terminal taxon (Fig. 13).

DESCRIPTION OF *ANNEMYS LEVENSIS*

Based on the available material, there are relatively few differences in the anatomy of *Annemys levensis* and *A. latiens*. We therefore chose to describe the better-preserved *A. levensis* first and to only highlight differences in the section on *A. latiens*.

Skull

The holotype and only known partial skeleton of *Annemys levensis* (PIN 4636-4) has an excellent, almost complete skull (PIN 4636-4-2; Fig. 1). It only lacks parts of the premaxillae, most of the quadratojugals, and the posterodorsal margin of the supraoccipital crest. Much of the left cheek is present as an isolated element.

In general, the skull is characterized by a triangular outline that is roughly 28% longer than wide, well-developed cheek and upper temporal emarginations, dorsolaterally facing, relatively large orbits with shallow lower rim, and a short preorbital region. When viewed laterally, the skull is flat and gradually slopes from the supraoccipital towards the nasals. The skull roof is decorated with very fine grooves and ridges, whereas the otic chamber and the lateral surface of the squamosals are smooth.

Cranial Scales—Scale sulci are well defined in PIN 4634-6-2 (Fig. 1A, B, K). We adopt the system of Gaffney (1996) and Sterli and de la Fuente (2013) developed for cranial scales of basal turtles. Scale Z is subdivided into two smaller scales arranged along the midline (following Sterli and de la Fuente, 2013), a broader, anterior that covers the prefrontals and the nasals, and a narrower, posterior one that covers the frontal processes and the medial margins of the prefrontals. Scale Y is unpaired, covers the middle of the frontal bones, and has a regular hexagonal shape. Scale G was most probably paired and its anterior half extends onto the frontals and the posterior half onto the parietals. Its posterior margin is deeply emarginated. The unpaired scale X has a regular pentagonal shape and is slightly smaller in size than scale Y. Scale A is unpaired and extends along the medial rim of the upper temporal emargination formed by the parietals. Its posterior limit is unclear. Posterolaterally, scale A meets a small and triangular paired scale that borders the anteromedial rim of the upper temporal emargination. We are unable to find the homolog for this scale using the system of Sterli and de la Fuente (2013) and it could be a neomorph. Anterolaterally, scale A contacts a paired trapezoidal scale that is restricted to the parietals and we tentatively interpret it as scale H. Lateral to this scale lies another paired scale extending onto the postorbital and slightly onto the parietals. We tentatively interpret it as scale D. Scale F is interpreted to be subdivided into at least four smaller scales following Sterli and de la Fuente (2013). They extend along the dorsal margin of the orbit from the posterodorsal to

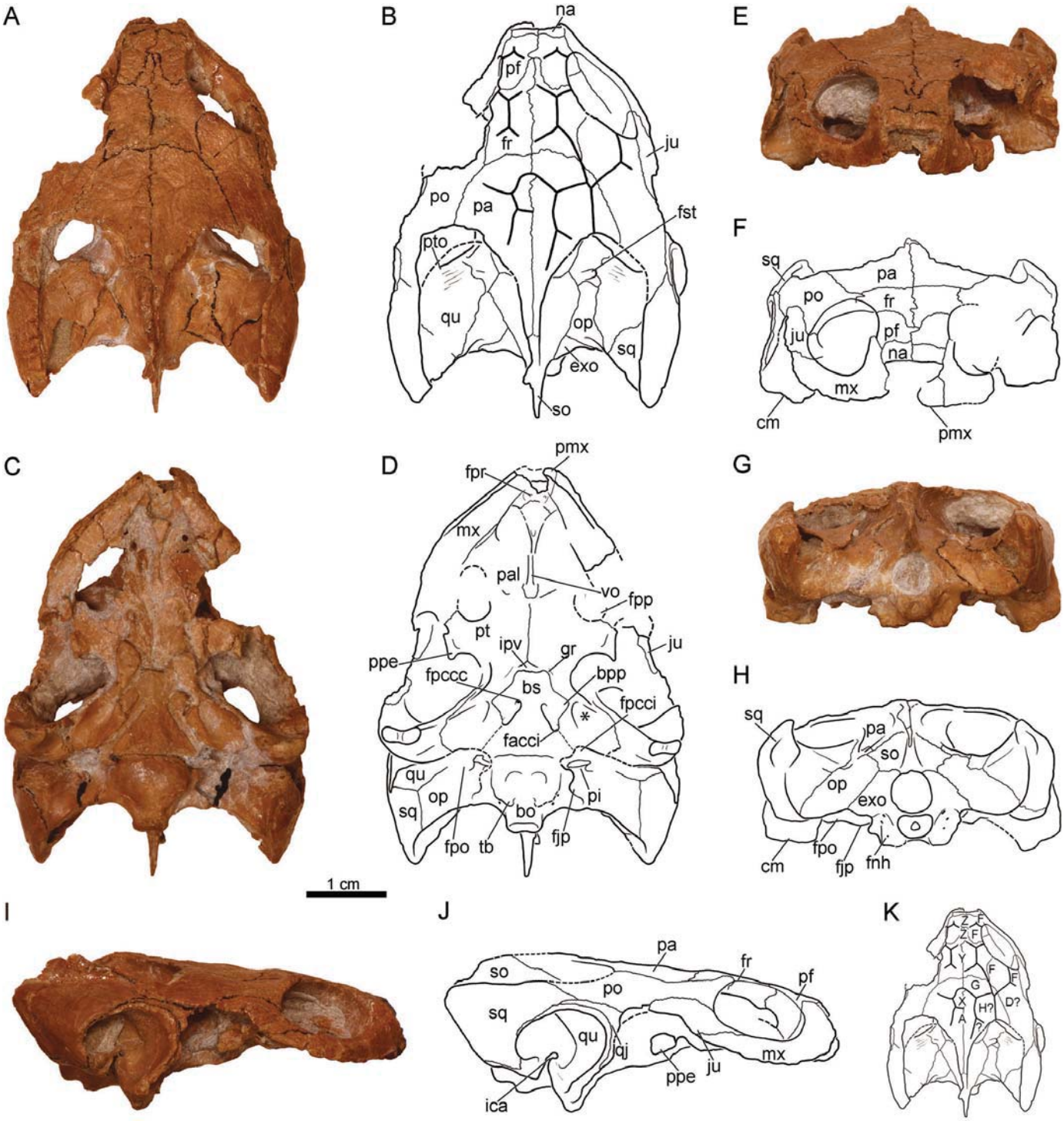

FIGURE 1. PIN 4636-4-2 (holotype), *Annemys levensis*, skull, Late Jurassic, Shar Teg, Ulan Malgait beds, Govi Altai Aimag, Mongolia. **A**, **B**, photograph and line drawing in dorsal view; **C**, **D**, photograph and line drawing in ventral view; **E**, **F**, photograph and line drawing in anterior view; **G**, **H**, photograph and line drawing in posterior view; **I**, **J**, photograph and line drawing in right lateral view; **K**, line drawing of skull roof scales. **Abbreviations**: **bo**, basioccipital; **bpp**, basipterygoid process; **bs**, basisphenoid; **cm**, condylus mandibularis; **exo**, exoccipital; **facci**, foramen anterius canalis caroticus internus; **fjp**, foramen jugulare posterius; **fnh**, foramen nervi hypoglossi; **fpccc**, foramen posterius canalis caroticus cerebralis; **fpcci**, foramen posterius canalis carotici interni; **fpo**, fenestra postotica; **fpp**, foramen palatinum posterius; **fpr**, foramen praepalatinum; **fr**, frontal; **fst**, foramen stapedio-temporale; **gr**, groove for palatine branch of the carotid; **ica**, incisura columella auris; **ipv**, interpterygoid vacuity; **ju**, jugal; **mx**, maxilla; **na**, nasal; **op**, opisthotic; **pa**, parietal; **pal**, palatine; **pf**, prefrontal; **pi**, processus interfenestralis; **pmx**, premaxilla; **po**, postorbital; **ppe**, processus pterygoideus externus; **pt**, pterygoid; **pto**, processus trochlearis oticum; **qj**, quadratojugal; **qu**, quadrate; **so**, supraoccipital; **sq**, squamosal; **tb**, tubera basioccipitalis; **vo**, vomer; **A**, **D**, **F**, **H**, **G**, **X**, **Y**, **Z**, cranial scales (following the terminology of Sterli and de la Fuente, 2013); *, pterygoid pit.

the anterodorsal corner. The largest is the third counting from the front and it contacts scales G and Y medially. The precise extent of the most posterior scale F remains unclear. Of the two anterior F scales, the second from the front is the larger and both form the lateral borders of the subdivided scale Z.

Nasals—A pair of small nasals is present that forms the dorsal margin of the apertura narium externa (Fig. 1A, B, E, F). The nasals have the shape of wide rectangles and their midline contact with one another is not interrupted by the frontals. The nasals contact the prefrontals posteriorly and the maxillae ventrolaterally.

Prefrontals—The dorsal plates of the prefrontals are subrectangular and roughly twice as long as wide (Fig. 1A, B, E, F). A clear medial contact of the prefrontals with one another is present along the anterior halves of these elements, but the anterior process of the frontals divides their posterior halves. The prefrontals form the anterior third of the dorsal rim of the orbits, meet the nasals anteriorly, the maxillae anterolaterally, and the frontals posteromedially. The descending process of the prefrontals defines the anterior wall of the orbit and the extensive development of the palatines along the floor of the orbit indicates that a distal contact of the descending process with the palatines must have been present, although it is currently not preserved. The great size of the descending process of the prefrontals furthermore evinces that a vomer-prefrontal contact is very likely present, but damage to this region obscures this contact as well. The foramen orbito-nasale is small, but badly preserved due to damage along the flooring of the fossa orbitalis, and it is therefore unclear if the prefrontals contribute to its margins.

Frontals—In dorsal view, the frontals have relatively short anteromedial processes that are about half of the length of the remaining part of these bones and only partially separate the prefrontals (Fig. 1A, B, E, F). The frontals form about one-third of the length of the dorsal orbital rim. In dorsal view, the frontals contact the prefrontals anterolaterally, the postorbital posterolaterally, and the parietals posteriorly. The olfactory region of the frontals is not visible, because the interorbital fossa is not prepared, but it is apparent that the prefrontals and frontals form a distinct sulcus olfactorius. It is unclear if the frontals contact the nasals within the roofing of the nasal capsule.

Parietals—The right parietal is preserved almost completely, including the rim of the upper temporal emargination, but excluding the posterior process along the supraoccipital crest (Fig. 1A, B, E, F). The left parietal, by contrast, is mostly damaged along the upper temporal emargination. The parietals are relatively broad elements that show long contacts with the postorbitals laterally and short, transverse contacts with the frontals anteriorly. Posteriorly, the parietals cover the anterior half of the supraoccipital crest but do not reach the level of the occipital condyle. The deepest point of the extensive upper temporal emargination is preserved by the right parietal and is located slightly anterior to the anterior border of the cavum tympani in lateral view, and anterior to the anterior wall of the otic chamber in dorsal view. Possible contacts with the squamosals cannot be verified due to the incompleteness of these elements, but if any were present, they must have been point-like contacts along the margin of the upper temporal emargination. The processus parietalis inferior broadly contacts the prootic within the upper temporal fossa and contacts the pterygoids and epipterygoids anterior to the foramen nervi trigemini to form a broad anterior braincase wall. The right side of PIN 4636-4-2 best demonstrates that the parietals form the anterodorsal margin of the foramen nervi trigemini (Fig. 2).

Jugals—Only the right jugal is completely preserved (Fig. 1A, B, E, F, I, J). The main body of the jugals forms much of the posteroventral margin of the orbit and contacts the maxilla anteriorly. The plate-like dorsal process, also preserved on the left side of the skull, contacts the postorbital dorsomedially. It appears

FIGURE 2. PIN 4636-4-2 (holotype), *Annemys levensis*, Late Jurassic, Shar Teg, Ulan Malgait beds, Govi Altai Aimag, Mongolia. Line drawing of the right trigeminal region of skull in lateral view, anterior is to the right. **Abbreviations**: **epi**, epipterygoid; **fnt**, foramen nervi trigemini; **pa**, parietal; **ppe**, processus pterygoideus externus; **pr**, prootic; **pt**, pterygoid; **qu**, quadrate.

that the jugal had a posterior point contact with the quadratojugal on the left side of the skull (not figured), but this is not certain, given that this region of the skull is badly damaged. A relatively deep lower temporal emargination is present, which reaches the midlevel of the orbit in lateral view. It is unclear whether the ventral plate contacted the posterior end of the triturating surface and the anterolateral tip of the external pterygoid process.

Quadratojugals—Only the dorsal portions of the quadratojugals are preserved on both sides of the skull, the right one being more complete (Fig. 1I, J). These remnants are wedged between the postorbital dorsally and the dorsal rim of the cavum tympani ventrally and narrowly contact the squamosal posteriorly. It appears that a small fragment of the left quadratojugal contacts the dorsal process of the jugal anteriorly, but damage to this region of the skull makes this contact all but certain. The articular surface for the quadratojugal along the anterior rim of the cavum tympani (i.e., the quadrate) is nicely preserved on the right side of the skull and reveals that the ventral aspect of the quadratojugals almost reaches the level of the articular condyles ventrally.

Squamosals—The squamosals are cone-shaped elements that form the roof of the inflated antrum postoticum and the posterolateral margins of the upper temporal fossa (Fig. 1). In lateral view, the squamosals have an extensive contact with the quadrates dorsally and posteriorly to the cavum tympani. It sits on the cavum tympani of the quadrate but does not contribute to the actual rim of the cavum tympani. The squamosals furthermore have a short anterior contact with the quadratojugals and a broader contact with the postorbital. Within the upper temporal fossa, the squamosal contacts the paroccipital process of the opisthotic ventromedially and laps onto the quadrates anteromedially. Anterior point contacts with the parietals may have been present along the anterior margin of the upper temporal

emargination, but an actual contact is not preserved on either side of the skull. The posterior tips of the squamosals are rounded and reach posteriorly beyond the level of the occipital condyle but not as far as that of the supraoccipital crest. The lateral surface is smooth and lacks clear muscle attachment sites.

Postorbitals—The postorbitals are anteroposteriorly elongated elements that cover much of the midlateral aspects of the skull and form the posterior margin of the orbits (Fig. 1A, B, I, J). The width of the postorbitals is slightly greater than that of the frontals. Posteromedially, the postorbitals contact the parietals along sutures that are about twice as long as the anteromedial contacts with the frontals. The postorbitals are perhaps excluded from the lower temporal emargination by a jugal-quadratojugal contact and from the upper temporal emargination by a squamosal-parietal contact, but damage to all relevant regions of the skull prohibit confident assessment of this morphology. The postorbital has no contact with the palatine.

Premaxillae—Only fragments of both premaxillae are preserved, the left one being more complete (Fig. 1F). The premaxillae form the ventral border of the external narial opening and the anterior portion of the labial ridge. They contact the maxilla posterolaterally and the vomer posteriorly, but the latter contact is partially obscured by compression. The foramina praepalatinum are located on the ventral surface of the premaxilla and do not appear to have a contribution from the vomer. A distinct premaxillary hook is absent.

Maxillae—The maxillae, as preserved on the right side of the skull, and disarticulated on the left side, form narrow, slightly curved, and parallel-sided triturating surfaces (Fig. 1A–D). A sharp labial ridge is present, whereas only hints of a lingual ridge are apparent near the palatine contacts. The palatines, jugals, and vomer are not involved in the triturating surfaces. In palatal view, the maxillae contact the premaxillae anteriorly, the vomer anteromedially, and the palatines medially. Ventrally, the posterior parts of the maxillae are not well preserved and potential posterior contacts with the pterygoids are therefore uncertain. A secondary palate is not developed.

The margins of the foramen palatinum posterius are uncertain because of rather extensive damage to this region of the skull. The distribution of palatine fragments along the middle third of the maxillae only, however, reveals that the foramen palatinum posterius was large in size. The foramen was defined by the maxillae laterally, the palatines medially, and the pterygoids posteriorly.

Lateral to the anterior wall of the orbits, the dorsal process of the maxillae overlap the descending process of the prefrontals and contact the nasals and the prefrontals medially. The maxillae form the anterior margins of the orbits, but their contribution to the anterior orbit walls is only minor. The foramen orbito-nasale is too poorly preserved to allow discerning whether the maxillae contribute to it. The lateral plate of the maxilla forms the lower rim of the orbit and is posterodorsally overlapped by the jugal.

Vomer—The vomer is damaged in PIN 4636-4-2 but enough is preserved to describe the most important features (Fig. 1C, D). This element is narrow and crest-like, has widened anterior and posterior ends, and separates the choanae. The anterior part of the vomer is broken and displaced dorsally relative to the main body of the bone together with the crushed premaxillary region. This portion nevertheless shows a clear anterior contact with the premaxillae and anterolateral contacts with the maxillae. Posteriorly, the vomer separates the palatines in ventral view and likely contacted the pterygoids as well. Although not visible directly, a contact with the prefrontal must have been present, as can be deduced from the extensive descending process of the prefrontal.

Palatines—The palate is compressed and the palatines are better preserved on the left side of the skull (Fig. 1C, D). Anterolaterally, the palatines touch the maxillae along the low lingual ridge of the triturating surface. The palatines form the medial and anterior margins of the damaged foramen palatinum posterius and medially contact the vomer. It is difficult to discern if the palatines contact one another in ventral view posterior to the vomer because this region is only poorly prepared, but the vomer likely separates the palatines from one another by contacting the pterygoid. It is also unclear if the palatines perhaps contacted one another dorsally within the interorbital foramen. The posterior suture between the palatines and the pterygoids is concave posteriorly and the posterolateral edge of the palatine is at the level of the foramen palatinum posterius.

Quadrates—The quadrates contact within the otic region the squamosals posterolaterally, the opisthotics posteromedially, and the prootics anteromedially (Fig. 1). The stapedial foramen, better preserved on the right side of the skull, is well developed and located in the anteromedial region of the roof of the otic chamber. The lateral margin of the foramen is defined by the quadrate, whereas the medial margin and a shallow, exiting groove are formed by the prootic. The presence of an unambiguous processus trochlearis oticum cannot be identified confidently because there is no prominent protrusion. The anterodorsal margin of the quadrate along the anterior margin the otic chamber nevertheless exhibits a slightly raised rugose area that probably held a cartilage that helped redirect the adductor musculature. The prootic does not participate in this structure.

The tympanic region of the quadrate is in clear contact with the quadratojugal anterodorsally and the squamosal posterodorsally. The ventral portions of the quadratojugals are damaged, but an additional anterior quadratojugal contact is evidenced by sutural margins. The antrum postoticum is well developed and the cavum tympani is deep and has a kidney-shaped outline in lateral view. No precolumellar fossa is present within the cavum tympani, but a shallow, oval-shaped embayment is apparent just dorsal to the quadrate condyle. The posterior margin of the cavum tympani is formed by the quadrates, not the squamosal. The full outline of the cavum tympani would therefore be preserved if the squamosals were removed. The incisura columella auris is very narrow, but not posteriorly enclosed, and a small fragment of the elegant stapes is preserved within the incisura on the left side of the skull.

The ventral portions of the quadrates contact the pterygoids medially and the epipterygoid anteriorly and form condyli mandibularis that are situated well anteriorly to the condylus occipitalis. The articular processes are rather low and the entire skull therefore has only a low height. The mandibular condyles are anteroposteriorly short and oriented slightly to the anterior.

Epipterygoids and Trigeminal Area—The epipterygoids are laminar elements best preserved on the right side of the skull (Fig. 2). They contact the pterygoids ventrally and form the ventral and the anterior margins of the trigeminal foramen. The posterior margin of the trigeminal foramen is formed by the pterygoid and the dorsal margin by the prootic, but here an elegant and laminar posterior process of the parietal overlaps the prootic. However, the internal dorsal margin is clearly formed by the prootic. Posteriorly, the epipterygoid is bordered by an element that is possibly a thin lamina of the quadrate overlapping the pterygoid. Along the ventral edge of the bone there is a thickened laterally protruding lip.

Pterygoids—The pterygoids send long processes posterolaterally that surround the basisphenoid laterally, reach the back of the skull without contacting the basioccipital, and lap onto the quadrate rami (Figs. 1B, 2). The cavum acustico-jugulare is fully floored by these elements and the prootics are therefore not visible in ventral view. At the back of the skull, part of the floor of the canalis carotici interni is eroded away (contra Sukhanov [2000], who interpreted the canals are being primarily exposed). However, this erosion makes it apparent that the canal extends from the foramen posterius canalis carotici interni to the unfloored carotid sulcus of the basisphenoid and is formed along

the contact of the pterygoids and the basisphenoid. The exact position of the foramen posterius canalis carotici interni is unclear, but it must have been placed at the posterior end of the pterygoid (now eroded) in line with the carotid canal. The basisphenoid might have been excluded from the formation of this foramen. Medially to the quadrate ramus the pterygoids have large, shallow, oval depressions, the fossae pterygoidei. At the anteromedial margin of the depression, the pterygoids articulate with the basipterygoid processes of the basisphenoid. Anteriorly, the pterygoid rami form flat, rectangular plates that meet each other along the midline to form part of the primary palate. The posterior margin of these plates together with the anterior portion of the pterygoid rami and the anterior margin of the basisphenoid define a small rectangular space. Even though the pterygoids are compressed in this region and the anterior portion of the right ramus of the pterygoid is slightly displaced, the intact margins of all bones involved indicate that this space is bordered by natural, bony margins and we therefore identify it as a narrow remnant of the interpterygoid vacuity. More specimens of *A. levensis* or similar species may reveal in the future that this gap closes completely in later ontogenetic stages (e.g., as in *Xinjiangchelys radiplicatoides* where the entry of the palatine artery is represented by a pair of slit-like openings; Brinkman et al., 2013). A pair of grooves is formed by the quadrate ramus of the pterygoids that lead to the posterolateral corners of the remnant of the interpterygoid vacuity and it is evident that these held the palatine arteries. The area of the interpterygoid vacuity is too poorly preserved, however, to reveal if incipient foramina posterius canalis caroticus lateralis for the palatine arteries were present laterally; therefore, it remains unclear whether the palatine branch entered the skull via the vacuity or an adjacent foramen. If the latter case were true, the vacuity had already lost its function at this evolutionary stage of transmitting the palatine branch, but had not yet closed completely.

Anterolaterally, the pterygoids form the processus pterygoideus externus. The processus has a clearly developed vertical plate and a posterior process that protrudes into the lower temporal fossa. Anterolaterally to the processus pterygoideus externus, the pterygoids contact the maxillae and form the posterior rim of the foramen palatinum posterius. The pterygoids meet the palatines anteriorly, but it is uncertain if midline contacts of the palatines prohibit an anterior contact with the vomer.

In the trigeminal area, the dorsal plate of the pterygoid contacts the epipterygoid dorsally, the quadrate posterodorsally, and forms the posterior margin of the trigeminal foramen (Fig. 2).

Supraoccipital—The supraoccipital only lacks the posterodorsal portions of the supraoccipital crest (Fig. 1A, B). It contacts the parietals anterodorsally, the prootics anterolaterally, the opisthotics posterolaterally, and the exoccipitals posteriorly along the dorsolateral margin of the foramen magnum. The supraoccipital does not contribute to the foramen stapediotemporale. The posterodorsal portion of the supraoccipital crest is slightly damaged, but the posterior tip is intact and the crest extends slightly beyond the tips of the squamosals and occipital condyle. The preserved portion of the supraoccipital crest is laminar and lacks ridges.

Exoccipitals—The exoccipitals form the lateral and ventral margins of the foramen magnum (Fig. 1G, H). Dorsally, they contact the supraoccipital, laterally the opisthotic, and ventrally the basioccipital. Anteroventrally, the exoccipitals are incomplete on both sides and a contact with the pterygoid might have been present accordingly. The exoccipitals form the posterior wall of the recessus scalae tympani, but are not developed extensively enough to separate the foramen jugulare posterius from the fenestra postotica. Three pairs of small foramina nervi hypoglossi are present that are arranged in a roughly dorsoventrally directed curve and that decrease in diameter ventrally. The exoccipitals are fully fused with the basioccipital.

Basioccipital—The basioccipital is fused with the exoccipitals dorsally and most probably forms the occipital condyle with these bones (Fig. 1C, D). An anterior, transverse contact is present with the basisphenoid. A deep groove is apparent between these two bones, and although this area is eroded, its rugose surface is indicative of being a true anatomical structure. Ventrally, the basioccipital and/or exoccipital form a pair of tubercula basioccipitale. A shallow heart-shaped depression dominates the ventral surface of the basioccipital that does not extend onto the basisphenoid.

Prootic—In dorsal view, the prootics are in contact with the parietal anteromedially, the supraoccipital posteromedially, the opisthotic posteriorly, and the quadrate laterally (Figs. 1A, 2). The prootics form the medial portion of the large foramen stapedio-temporale and the anteromedial wall of the otic chamber. They lack a rugose surface along the anterodorsal side of the otic wall and are therefore inferred to not have participated in the formation of a processus trochlearis oticum. The prootics form the inner dorsal margin of the trigeminal foramen, but the external margin is overlapped by a posterior narrow lamina of the parietal.

Opisthotic—The opisthotics contact the quadrates anterolaterally, the squamosals posterolaterally, the exoccipitals posteromedially, the supraoccipital medially, and the prootics anteriorly (Fig. 1A, B, C, D, G, H). A ventral process of the opisthotic, the processus interfenestralis, separates the recessus scalae tympani from the cavum acustico-jugulare and the cavum labyrinthicum. The distal portion of the processus interfenestralis expands to form a small horizontal plate that does not completely reach the ventral surface of the basicranium but narrowly contacts the dorsal surface of the posterior tip of the pterygoid and the basisphenoid and even the anterolateral edge of the basioccipital. The processus interfenestralis remains fully visible in ventral view, at least as preserved. However, this area is damaged and the exoccipital possibly covered it ventrally to an extent that the process may not have been visible at all. At the dorsal base of the right processus, a small foramen is present, the foramen internum nervi glossopharyngei. The fenestra perilymphatica is large and allows communication between the recessus scalae tympani and the cavum labyrinthicum. The cavum acustico-jugulare posteriorly opens into the large fenestra postotica that is defined by the opisthotics dorsally and dorsolaterally, the quadrates anterolaterally, the pterygoids and the basisphenoid anteriorly, and the basi- and exoccipitals medially.

Basisphenoid—The basisphenoid is slightly damaged posteriorly and lacks the flooring of the internal carotid canals (Fig. 1C, D). The basisphenoid is longer than wide and tapers and widens anterior and posterior to the basipterygoid processes, respectively. The basisphenoid meets the basioccipital posteriorly via a transverse suture, contacts the pterygoids laterally, and contributes to the fenestra postotica. Well-developed basipterygoid processes are present that project laterally from the anterior half of the basisphenoid to fit into the corresponding pockets of the pterygoids. The processes are flat, triangular in outline, and roughly as long as they are wide. The basisphenoid has a transverse, anterior free margin that defines the posterior border of the reduced interpterygoid vacuity. The foramen posterius canalis carotici interni is damaged but opened at the back of the skull either between the basisphenoid and the pterygoid or within the pterygoid only. The flooring of the canalis carotici interni and the posterior entry of the canal was formed by the pterygoids and basisphenoid, but is now eroded. It former presence, however, is indicated by residual fragments and broken margins. Intact margins at the level of the basipterygoid process combined with exposed posterior foramina of the cerebral artery reveal that the split of the carotid artery into cerebral and palatine branches was not floored, as in sinemydids and other xinjiangchelyids. The anterior foramen of the internal carotid artery and the posterior

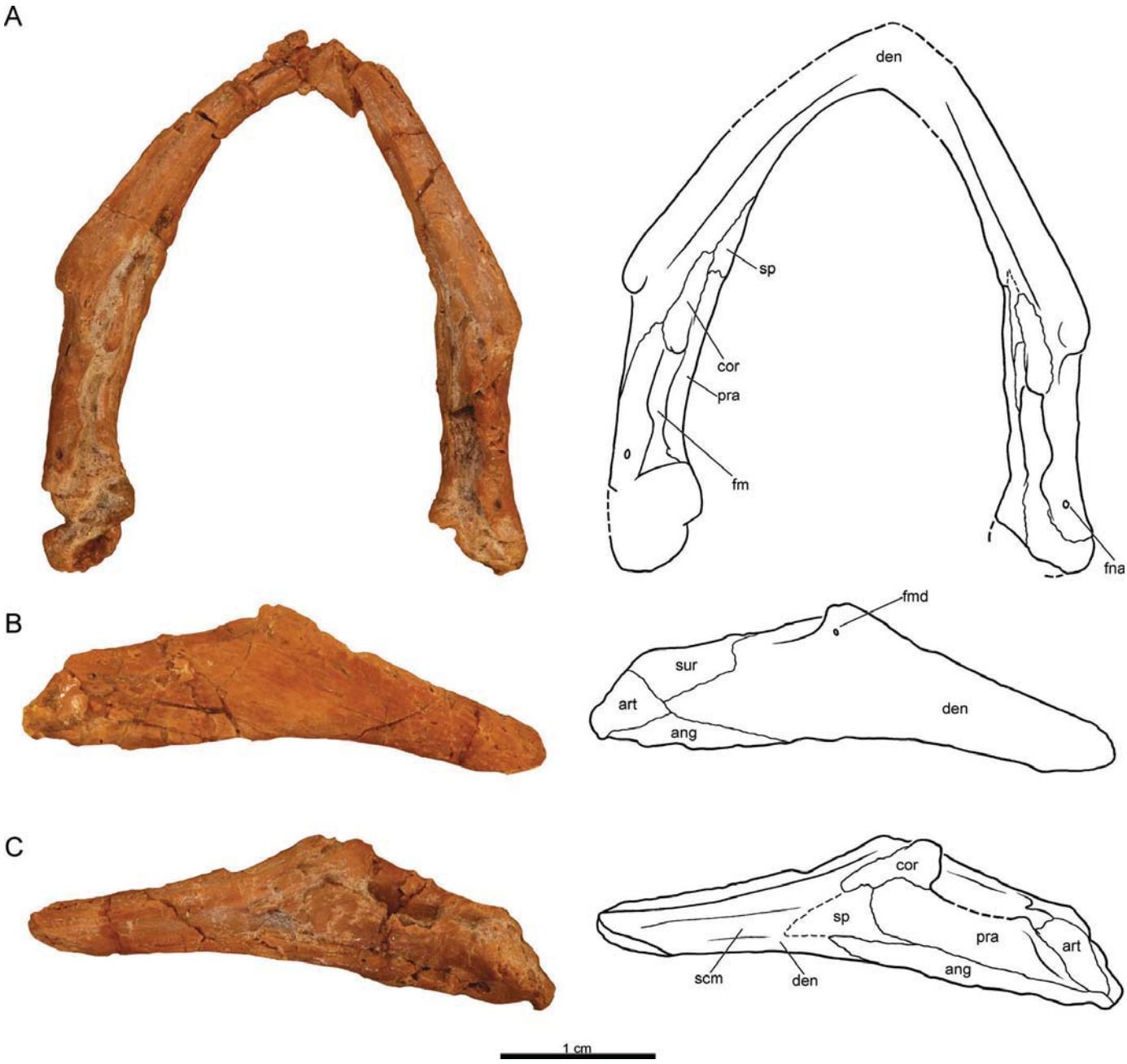

FIGURE 3. PIN 4636-4-2 (holotype), *Annemys levensis*, mandible, Late Jurassic, Shar Teg, Ulan Malgait beds, Govi Altai Aimag, Mongolia. **A**, photograph and line drawing in dorsal view; **B**, photograph and line drawing of right ramus in lateral view; **C**, photograph and line drawing of right ramus in medial view. **Abbreviations**: **ang**, angular; **art**, articular; **cor**, coronoid; **den**, dentary; **fm**, fossa Meckelii; **fmd**, foramen dentofaciale majus; **fna**, foramen nervi auriculotemporalis; **pra**, prearticular; **scm**, sulcus cartilaginis Meckelii; **sp**, splenial; **sur**, surangular.

foramen of the cerebral artery are connected by a marked sulcus. A pair of incipient foramina posterius canalis carotici lateralis may have been present along the suture with the pterygoid just lateral to the interpterygoid vacuity. Paired pits on the ventral surface of the basisphenoid are absent.

Mandible

An almost complete, delicate lower jaw is associated with the skull (Fig. 3). It is characterized by a narrow and relatively elongate triturating surface with sharp labial and lingual ridges, a low coronoid process, and a short retroarticular process. The symphysis is damaged and the presence of a midline hook therefore remains unclear, but enough is preserved to tell that the dentaries were fused. On the right side, the posterior fragment of the splenial is visible wedged between the coronoid, prearticular, and angular. The foramen dentofaciale majus is situated just below the posterodorsal corner of the triturating surface on the lateral wall of the dentary. A small foramen nervi auriculotemporalis is present on the posterior region of the surangular.

Shell

PIN 4636-4-1 is a shell found associated with the PIN 4636-4-2 skull (Figs. 4, 5). It only lacks the right peripherals 9–11, the left peripherals 7–9, and the pygal.

Carapace—The carapace is 325 mm long, low, and suboval and reaches its greatest width at the level of peripheral 8 (Fig. 4). The surface texture of the shell is generally smooth, with the exception of poorly defined outward radiating low plications on the anterior halves of the vertebrals. The nuchal is trapezoidal, about twice as wide as long, and has a distinct emargination that involves peripheral 1. Costiform processes are clearly absent. There are eight neurals, of which most are hexagonal with short sides facing anterolaterally, with the exceptions of neurals 1 (elongated, quadrangular), 7 (short oval), and 8 (short, hexagonal). The neural series is interrupted posterior to neural 6, allowing for a midline contact of costal 7 and resulting in a reduced neural 7. There are eight pairs of costal bones. Costal 1 is subtrapezoidal in shape and tapers laterally. Its anteroposterior length is not greater than that of the other costals. Costals 1–3 slightly bend anteriorly and costals 1 and 2 show a slight anterior concavity. Costal 4 is oriented perpendicular to the midline, costals 5 and 6 are slightly bent to the posterior, and costals 7 and 8 are strongly bent to the posterior (Fig. 4A). Dorsal ribs 2–9 have flat and triangular distal free ends that fit into corresponding sockets in the peripherals. The rib ends of dorsal ribs 1–8 are neither visible on the dorsal or visceral side of the carapace due to the lack of carapacial fontanelles, but those of dorsal ribs 9 and 10 are visible in ventral view. On the right side of PIN 4636-4-1, dorsal rib 1 is preserved and anteriorly overlaps the margin of dorsal rib 2, whereas laterally it extends roughly to the distal fifth of costal 1. Although dorsal rib 1 is shorter than that of *Hangaiemys* (*Kirgizemys*) *hoburensis* and *Sinemys lens*, the character definition of Joyce (2007) nevertheless requires that we score this taxon as having a 'long' dorsal rib 1, because it spans more than half the length of the costal. The second dorsal rib inserts only into the posterior third of peripheral 3. Dorsal rib 10 inserts into a groove in peripheral 11 on the visceral side of the carapace. The ilial articulation surface is visible on the visceral side of costal 8 (Fig. 4B).

Although the specimen is incomplete, we are confident that 11 pairs of peripherals were present and we number the posterior peripherals accordingly. A distinct gutter extends along the dorsolateral perimeter of the peripheral ring from the posterior half of peripheral 1 to at least peripheral 7 (Fig. 4A). Peripherals 7–11 are laterally expanded compared with the more anterior ones and peripherals 10 and 11 are slightly longer than wide (see a more detailed description of isolated peripherals of *Annemys* sp. from Shar Teg below).

Dorsal vertebrae 1–3, 5, 7, and 8 are preserved in situ in the specimen; they are narrow and bear a low ventral keel along their centra. Dorsal vertebra 1 is about half as long as dorsal vertebra 2. The anterior articulation of the centrum faces anteriorly and slightly ventrally and there are no signs of ventrally curving zygapophyses. The space between the distal portion of the dorsal ribs and the carapace is reduced (Fig. 4B).

Two suprapygals are present, the anterior one being trapezoidal and slightly wider than long and the posterior being very wide and short with biconvex lateral corners. Together with costal 8, suprapygal 2 excludes suprapygal 1 from contacting the peripherals (Fig. 4A).

Carapacial Scales—A wide cervical scale is present that covers the anterior half of the nuchal. There are five narrow vertebrals, the widest being vertebral 1, which is trapezoidal in shape, wider than long, and does not extend onto the peripherals. Vertebral 2 is hexagonal and longer than wide, vertebral 3 is hexagonal and as long as wide, and vertebral 4 is hexagonal and slightly wider than long with angular lateral corners. The sulcus between vertebrals 3 and 4 crosses the anterior third of neural 6. Vertebral 5 is wider than long, covers both suprapygals, slightly extends onto peripheral 11, and probably also onto the pygal, although this portion of the shell is not preserved.

The pleurals are about twice as wide as long and they cover much of the costals. Pleural 1 barely overlaps onto peripherals 1–3 and pleurals 2 and 3 extend onto peripherals 8–11.

There were 12 marginal scales, of which marginals 4–7 extend onto the costals, whereas the rest is restricted to the peripherals. The condition is unclear for marginal 8, because the relevant bones are not preserved. From the posterior half of peripheral 5 to peripheral 7, the sulcus between the marginals and the pleurals extends parallel to the border between the peripherals and the costals (Fig. 4A).

Plastron—The plastron is completely preserved and was found in association with the PIN 4636-4-1 carapace (Fig. 5). It is well ossified, relatively thick, and moderately extensive with a slightly short, wide, anteriorly tapering anterior lobe and a more elongated, narrow, posteriorly tapering posterior lobe. The plastron is thickened at the level of the base of the axillary and inguinal buttresses and along the lateral margin of the posterior lobe. The epiplastra meet one another on the midline, are pentagonal in outline, have rounded anterolateral margins, and almost parallel and transverse anterior and posterior borders. The anterior margin of the plastron is therefore nearly transverse. On the dorsal side of the epiplastra, remnants of the paired dorsally directed epiplastral processes (not cleithra sensu Joyce et al., 2006) are visible in the posteromedial corners of the elements, close to the suture with the entoplastron. In ventral view, the entoplastron is pentagonal, nearly twice as long as wide and its convex anterior margin partially separates the epiplastra from contacting one another. It is tightly sutured with the epiplastra and the hyoplastra via vertical, finely serrated sutures (Fig. 5A). In dorsal view, the entoplastron is more elongated and narrow than in ventral view, tapers posteriorly, and laterally extends a pair of finger-like processes to contact the hyoplastra. It contacts the epiplastra via an inverted 'V'-shaped suture. The interclavicular portion of the entoplastron extends in the form of a low median ridge along the slightly concave surface of the dorsal side of the entoplastron (Fig. 5B). The hyoplastron forms the relatively wide base of the anterior lobe and contributes to the anterior half of the bridge. The plastron contacted the carapace via pegs and ligaments that insert into pits on the peripherals that are aligned into a ventromedially oriented row. The contacts of the axillary and inguinal buttresses appear to be stronger than those of the remaining parts of the bridge. The axillary buttress is moderately developed and contacts the carapace from the posterior half of peripheral 2 to the posterior end of peripheral 3, but does not contact costal 1 (Fig. 4B). The broken distal end of the right axillary buttress is preserved in situ in articulation with the carapace (Fig. 4B). An anterior and a posterior musk duct foramen are present on both hyoplastra and at least one musk duct foramen is present along the anterior portion of the hypoplastron. Mesoplastra are absent. The hypoplastra form the posterior half of the bridge and the relatively narrow base of the posterior lobe. Three pegs for the carapace attachment are preserved on the left side (Fig. 5A). The inguinal buttress terminates on the anterior third of peripheral 8. The distal end of the left inguinal buttress is found displaced on the visceral side of costal 5 (Fig. 4B). The distal portion generally resembles a free rib head in being flat, triangular, and by being ornamented with radiating striations.

The xiphiplastra form slightly more than half of the posterior lobe. An anal notch is absent (Fig. 5A). The dorsal side of the xiphiplastra shows a flat and oval articulation surface for the pubis.

Plastral Scales—There is one pair of gulars and one pair of extragulars. The extragulars are restricted to the epiplastron

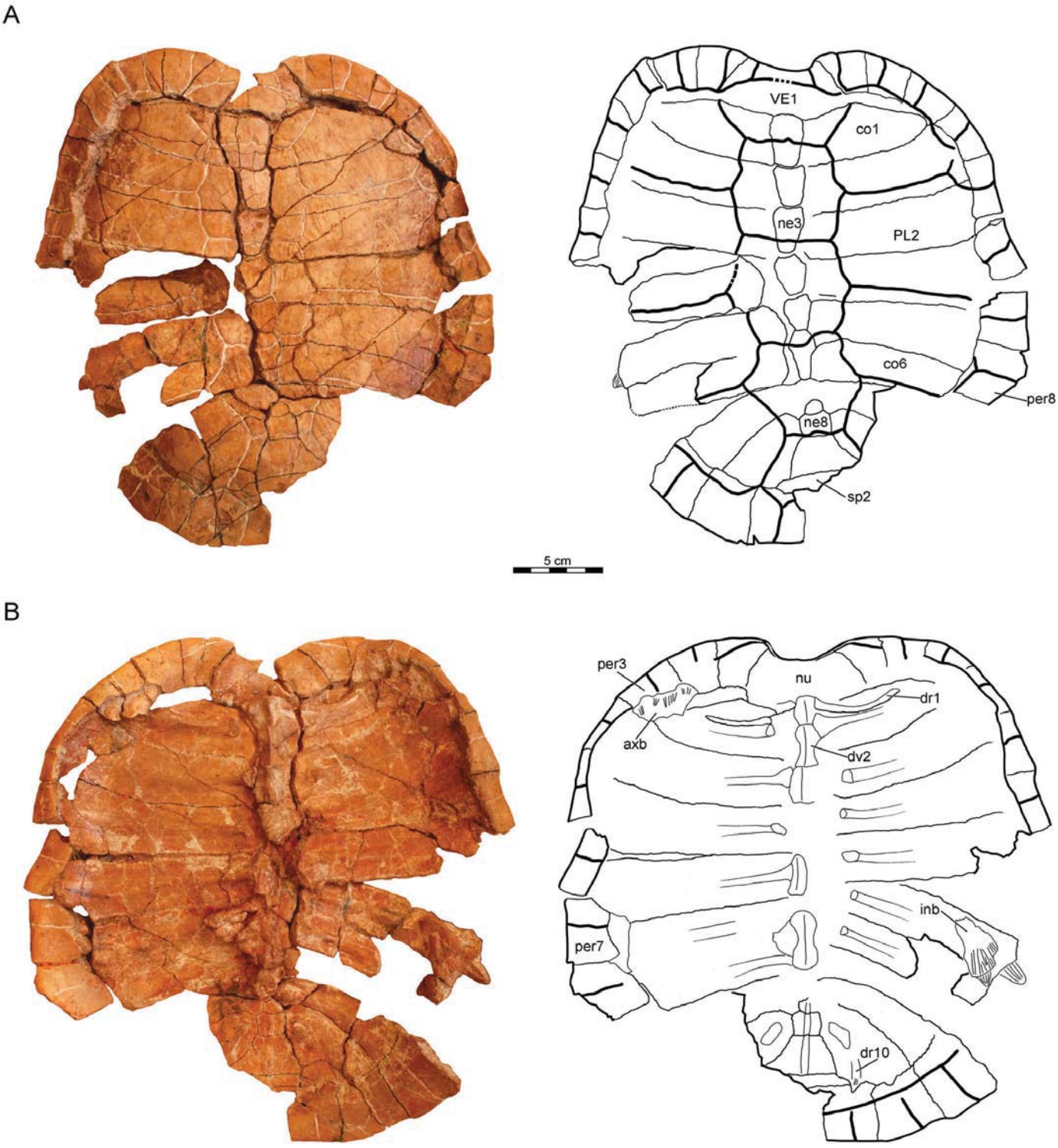

FIGURE 4. PIN 4636-4-1 (holotype), *Annemys levensis*, carapace, Late Jurassic, Shar Teg, Ulan Malgait beds, Govi Altai Aimag, Mongolia. **A**, photograph and line drawing in dorsal view; **B**, photograph and line drawing in ventral view. **Abbreviations**: **axb**, axillary buttress; **co**, costal; **dr**, dorsal rib; **dv**, dorsal vertebra; **inb**, inguinal buttress; **ne**, neural; **nu**, nuchal; **per**, peripheral; **PL**, pleural; **sp**, suprapygal; **VE**, vertebral.

and the left gular slightly extends onto the entoplastron. An asymmetric, aberrant scale and two short, aberrant blind sulci are present on the anterior region of the plastron. The midline sulcus is slightly sinusoidal and the humero-pectoral sulcus is positioned well posterior to the entoplastron. There are four pairs of inframarginals. They are relatively wide, restricted to the plastron, and do not extended on to the peripherals. The pectoral is slightly longer than the abdominal along the midline, but

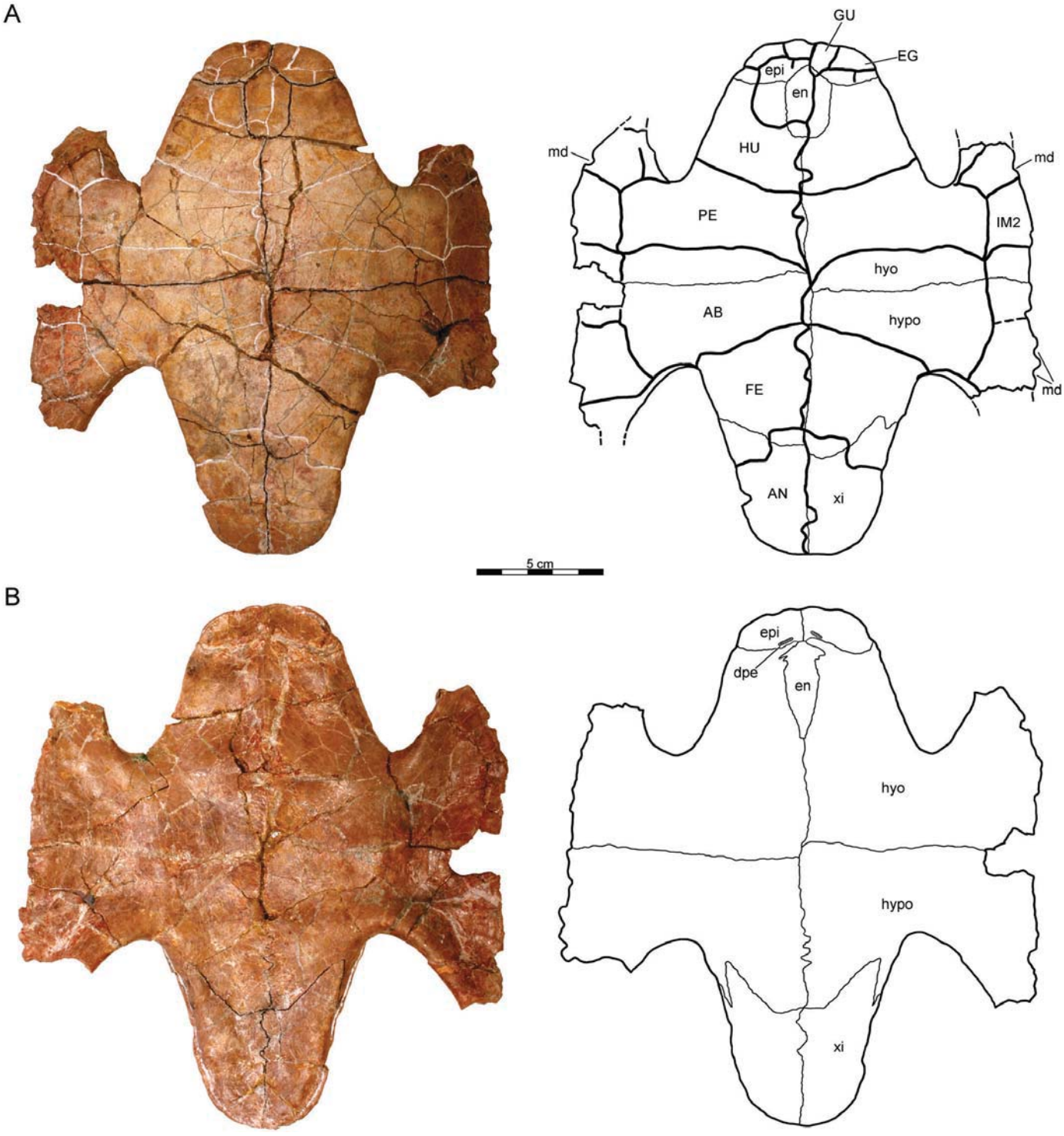

FIGURE 5. PIN 4636-4-1 (holotype), *Annemys levensis*, plastron, Late Jurassic, Shar Teg, Ulan Malgait beds, Govi Altai Aimag, Mongolia. **A**, photograph and line drawing in ventral view; **B**, photograph and line drawing in dorsal view. **Abbreviations**: **AB**, abdominal; **AN**, anal; **dpe**, dorsal process of epiplastron; **EG**, extragulars; **en**, entoplastron; **epi**, epiplastron; **FE**, femoral; **GU**, gular; **HU**, humeral; **hyo**, hyoplastron; **hypo**, hypoplastron; **IM**, inframarginal; **md**, musk duct foramen; **PE**, pectoral; **xi**, xiphiplastron.

significantly shorter than the abdominal laterally. The femoro-anal sulcus is omega-shaped, extends onto the hypoplastron, and covers about 60% of the length of the posterior lobe. The width of this extension makes up about 45% of the posterior lobe width at the base (Fig. 5A).

DESCRIPTION OF *ANNEMYS LATIENS*

Skull

The skull associated with the holotype of *Annemys latiens* (PIN 4636-5-2) is preserved in several fragments in poor condition and

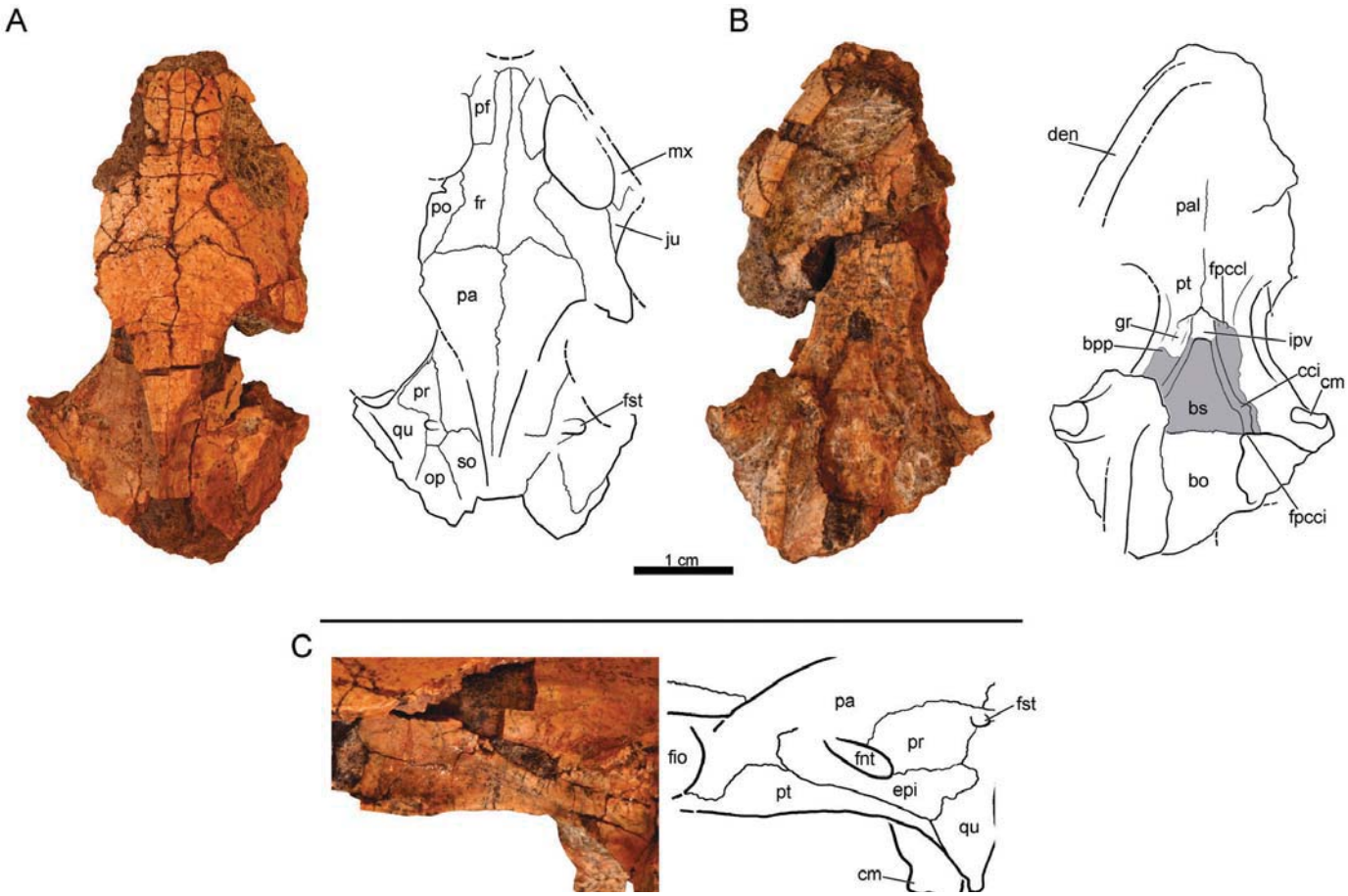

FIGURE 6. PIN 4636-6-1, *Annemys latiens*, skull, Late Jurassic, Shar Teg, Ulan Malgait beds, Govi Altai Aimag, Mongolia. **A**, photograph and line drawing in dorsal view; **B**, photograph and line drawing in ventral view; **C**, left trigeminal region in lateral view. **Abbreviations**: **bo**, basioccipital; **bpp**, basipterygoid process; **bs**, basisphenoid; **cci**, canalis caroticus internus; **cm**, condylus mandibularis; **den**, dentary; **epi**, epipterygoid; **fio**, foramen interorbitale; **fnt**, foramen nervi trigemini; **fpcci**, foramen posterius canalis carotici interni; **fpccl**, foramen posterius canalis carotici lateralis; **fr**, frontal; **fst**, foramen stapedio-temporale; **gr**, groove for palatine branch of carotid artery; **ipv**, interpterygoid vacuity; **ju**, jugal; **mx**, maxilla; **op**, opisthotic; **pa**, parietal; **pal**, palatine; **pf**, prefrontal; **po**, postorbital; **pr**, prootic; **pt**, pterygoid; **qu**, quadrate; **so**, supraoccipital. Gray color indicates eroded surfaces.

includes a partial left ramus of the lower jaw (not figured). The only informative part is the partial basicranium, which indicates that the skull could have been narrower than in *A. levensis*. The rostrum of the basisphenoid is anteriorly incomplete in this specimen, but it appears to be a flat structure. Dorsolaterally to the rostrum sits a pair of short and blunt processus clinoideus that appear to be damaged. The anterior opening of the canalis nervi abducentis is situated at the base of the processus clinoideus. The foramen anterior canalis carotici interni opens laterally to the sella turcica and its diameter is about half the size of the canalis cavernosus. The dorsum sellae slightly overhangs the sella turcica. What is preserved of the lower jaw is comparable to that of *A. levensis*.

PIN 4636-6-2 is an incomplete skull found associated with a partial *Annemys latiens* shell (Fig. 9; see below) that shows a number of distinct morphological characteristics that sharply differ from the skull of *A. levensis* (Fig. 6). The following cranial description focuses on the differences between the two species rather than repeating identical morphologies already described for *A. levensis* (see above).

PIN 4636-6-2 is missing the nasals and the premaxillae, the left maxilla, postorbital and jugal, the posterior end of the right postorbital, and the quadratojugals, squamosals, paroccipital processes, cava tympani, antra postoticum, exoccipitals, and the supraoccipital crest. The palate is largely obscured by matrix and the right dentary is still in articulation with the maxilla. The other dentary sits on the right side of the basicranial region. The ventral surface of the basisphenoid is extensively eroded revealing the canalis caroticus internus.

PIN 4636-6-2 strikingly differs from *Annemys levensis* in general proportions in being considerably more elongate and slender. This is best seen when the relative distance between the quadrate condyles are compared in the two skulls. This distance is approximately 30% less in PIN 4636-6-2 relative to *A. levensis*, even though the skulls have about the same anteroposterior length. Furthermore, the interorbital region of PIN 4636-6-2 is narrower and longer than that in *A. levensis*. The skull shape seen in the referred *A. latiens* skull is consistent with the narrow morphology seen in the holotype of this species (PIN 4636-5-2; see above). Cranial scales are not apparent.

Nasals—PIN 4636-6-2 lacks direct evidence for nasals, but a triangular space between the frontal and prefrontal is suggestive of the former presence of nasals (Fig. 6A). If this assertion were correct, the nasals would have been more trapezoidal shape in this specimen than in *A. levensis*.

Prefrontals—In PIN 4636-6-2, the prefrontals are fully separated from one another by the long anterior process of the frontals, unlike in *A. levensis* (Fig. 6A). This arrangement results in a more elongated shape for the prefrontals in *A. latiens* and slightly more extensive contributions of the prefrontals to the orbital rim relative to the frontals. The foramen interorbitale, the fossa orbitalis, and the fossa nasalis are completely obscured by matrix in this specimen.

Frontals—In PIN 4636-6-2, the anteromedial process of the frontal is longer, almost as long as the remaining parts of the bone and together with the more elongated prefrontal an extensive anteromedial process of the postorbital reduces the contribution of the frontals to the orbital margin relative to *A. levensis* (Fig. 6A). The long anteromedial process of the frontal in *A. latiens* probably also allowed a contact with the nasal, but this element is absent in the only available specimen. The interorbital space is narrower than in *A. levensis*.

Parietals—The parietals had a deep temporal emargination, but its precise extent cannot be clarified due to breakage. The inferior process of the parietal contributes to the dorsal margin of the trigeminal foramen (Fig. 6A).

Jugals—In PIN 4636-6-2, the jugal is present on the left side and its participation in the orbital margin is considerably reduced compared with *A. levensis* as a result of the expanded posterodorsal process of the maxilla (Fig. 6A).

Postorbital—In PIN 4636-6-2, the right postorbital is the least incomplete posteriorly. Both have considerably wider contacts (about twice) with the frontal compared with *A. levensis* thanks to the lateral constriction of the frontals caused by the anteromedial extension of the postorbitals. As a consequence of this, the frontal participation in the orbital margin is reduced in PIN 4636-6-2 relative to *A. levensis* (Fig. 6A).

Maxillae—The maxilla is incompletely preserved on the right side, although much of it is covered by the dentary (Fig. 6A). The maxilla has an expanded posterodorsal process that broadly contributes to the orbit and reduced the contribution of the jugal to the orbit relative to the condition seen in *A. levensis*. The triturating surface is narrow.

Pterygoids—A reduced interpterygoid vacuity is present at the anterior basisphenoid-pterygoid contact in *A. latiens*, similar to that of *A. levensis*. Just lateral to the remnant of the vacuity, still along the basisphenoid contact, there is a pair of incipient foramina, the foramen posterius canalis caroticus lateralis, that communicate with the interpterygoid vacuity and that likely held the palatal branch of the carotid artery (Fig. 6B). As in *A. levensis*, a narrow and shallow canal for the palatine branch of the carotid artery leads to this foramen that originated shortly after the fossa pterygoidea. It is possible that this foramen is present in the skull of *A. levensis*, but was obscured by poor preservation. The foramen posterius canalis carotici interni is not clearly discernable, but it was either formed by the pterygoid and the basisphenoid or solely by the pterygoid at the back of the skull.

Trigeminal Region—The foramen nervi trigemini is formed by the epipterygoid ventrally, the parietal anterodorsally, and the prootic posterodorsally (Fig. 6C). The epipterygoid is rod-like and the strong lip present in *A. levensis* is not apparent. The pterygoid contacts the quadrate posteriorly and it extends ventrally along the epipterygoid. The processus inferior parietalis of the parietal forms the posterior border of the foramen interorbitale and posteriorly it contacts the prootic. Unlike *A. levensis*, no posterior lamina of the parietal is apparent that would overlap the prootic just above the dorsal margin of the trigeminal foramen. There is no evidence of a laminar projection of the quadrate over the posterior half of the epipterygoid either. The pterygoid does not contribute to the posterior margin of the foramen, again unlike in *A. levensis*. These differences must be taken with caution because preservation and ambiguity with the interpretation of the *A. levensis* morphology make a clear comparison difficult.

Otic Region—Much of the cavum tympani and all of the antrum postoticum is missing. The incisura columella auris is slit-like. The quadrate bears with a modest processus trochlearis oticum in a form of a rugose surface (Fig. 6A). The contact of the opisthotic and the prootic hinders the quadrate from contacting the supraoccipital medially. The stapedial foramen opens on the dorsal face of the otic chamber and it is formed by the prootic and slightly by the quadrate. The supraoccipital contacts the opisthotic laterally, the parietal anteriorly, and the prootic anterolaterally.

Basisphenoid—The ventral surface of the basisphenoid is eroded and much of the floor of the canalis caroticus internus is missing. However, when complete, the canal most likely resembled the condition seen in *A. levensis* where only the posterior part of the canal is floored and the split for the palatine and cerebral branches of the carotid artery was not enclosed in bone. The paired basipterygoid process of the basisphenoid is tightly sutured to the corresponding 'pocket' of the pterygoid and it is horizontally oriented. Anteriorly, the basisphenoid terminates in a reduced interpterygoid vacuity that is clearly not the result of erosion. Laterally, the vacuity communicates with a pair of incipient foramen posterius canalis caroticus lateralis present along the basisphenoid-pterygoid contact. As best seen on the right side, a shallow groove leads to this foramen where the palatine branch must have extended. Our interpretation is that the palatine branch entered the skull via this foramen and that the vacuity already lost its function in transmitting the palatine branch at this evolutionary stage.

Shell

PIN 4636-5-1 (the holotype, not associated with the skull described above) is an incomplete shell lacking the right peripherals, the distal half of the right costals, both epiplastra, and parts of the bridge (Fig. 7). It resembles the shell of *A. levensis* in many respects and with the following description we intend to highlight the differences between the two species (most of them already reported in Sukhanov and Narmandakh, 2006).

Unlike in *A. levensis*, PIN 4636-5-1 lacks any ornamentation of the shell, but this might be a preservational artifact. The neural formula of the type specimen of *A. latiens* slightly differs from that of *A. levensis* in having a hexagonal neural 1, a quadrangular neural 2, and in being reduced to seven elements (Fig. 7A). Costal 7 sends a posterior process to contact the suprapygal hindering the midline contact of costals 8. Peripheral 1 is reduced and the nuchal excludes it from contacting costal 1. Vertebrals 2 and 3 are narrower in *A. latiens* and they are longer than wide. Marginals 4–8 overlap onto the costals, particularly marginal 5, as in *A. levensis*.

The plastron has a wider and shorter posterior lobe compared with that of *A. levensis* (Fig. 8). This is also evident from the difference in the relative proportions of the anal scale and the posterior lobe in the two species: in *A. levensis*, the anal scale does not reach the level of the transverse midline of the posterior lobe, whereas in *A. latiens* it extends to the midline (Fig. 8A). The axillary buttress may shortly contact the tip of costal 1 in addition to peripherals 2 and 3 (Fig 7B). In *A. levensis*, the contact with costal 1 is not apparent.

PIN 4636-6-1 is a partial shell preserving the plastron (posteriorly incomplete), the left peripherals 1–9, and the distal parts of costals 1–7 (Fig. 9). The PIN 4636-6-2 skull (see above; Fig. 6) is associated with this shell. We assign this shell (together with the skull) to *A. latiens* based on the presence of a wide posterior lobe and this attribute is confirmed by similarities in the skull. PIN 4636-6 may have a considerably wider entoplastron than all other *Annemys* specimens from Shar Teg, but preservation hinders an unambiguous determination of the original shape of this element.

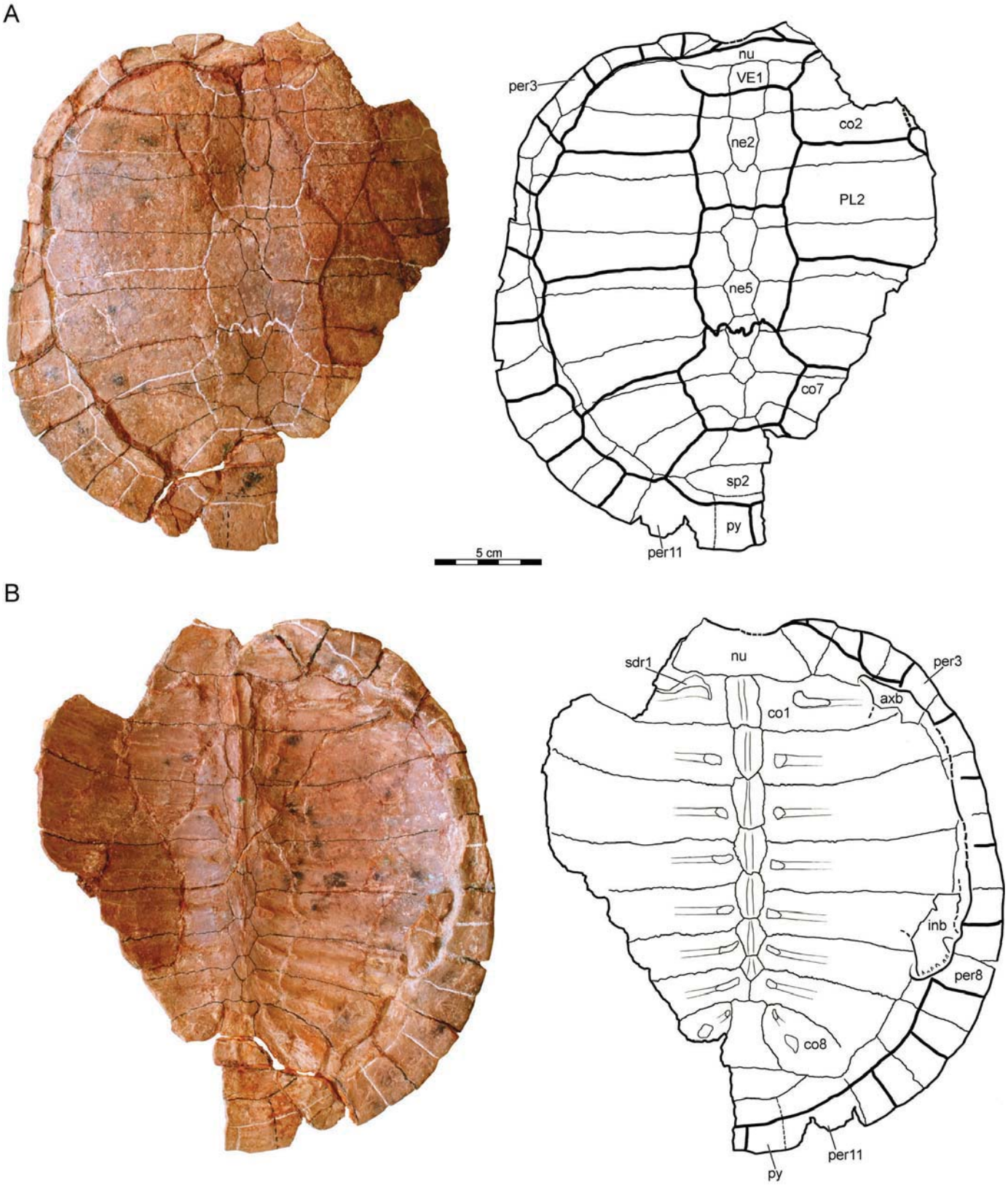

FIGURE 7. PIN 4636-5-1 (holotype), *Annemys latiens*, carapace, Late Jurassic, Shar Teg, Ulan Malgait beds, Govi Altai Aimag, Mongolia. **A**, photograph and line drawing in dorsal view; **B**, photograph and line drawing in ventral view. **Abbreviations**: **axb**, axillary buttress; **co**, costal; **inb**, inguinal buttress; **ne**, neural; **nu**, nuchal; **per**, peripheral; **PL**, pleural; **py**, pygal; **sdr**, scar for dorsal rib; **sp**, suprapygal; **VE**, vertebral.

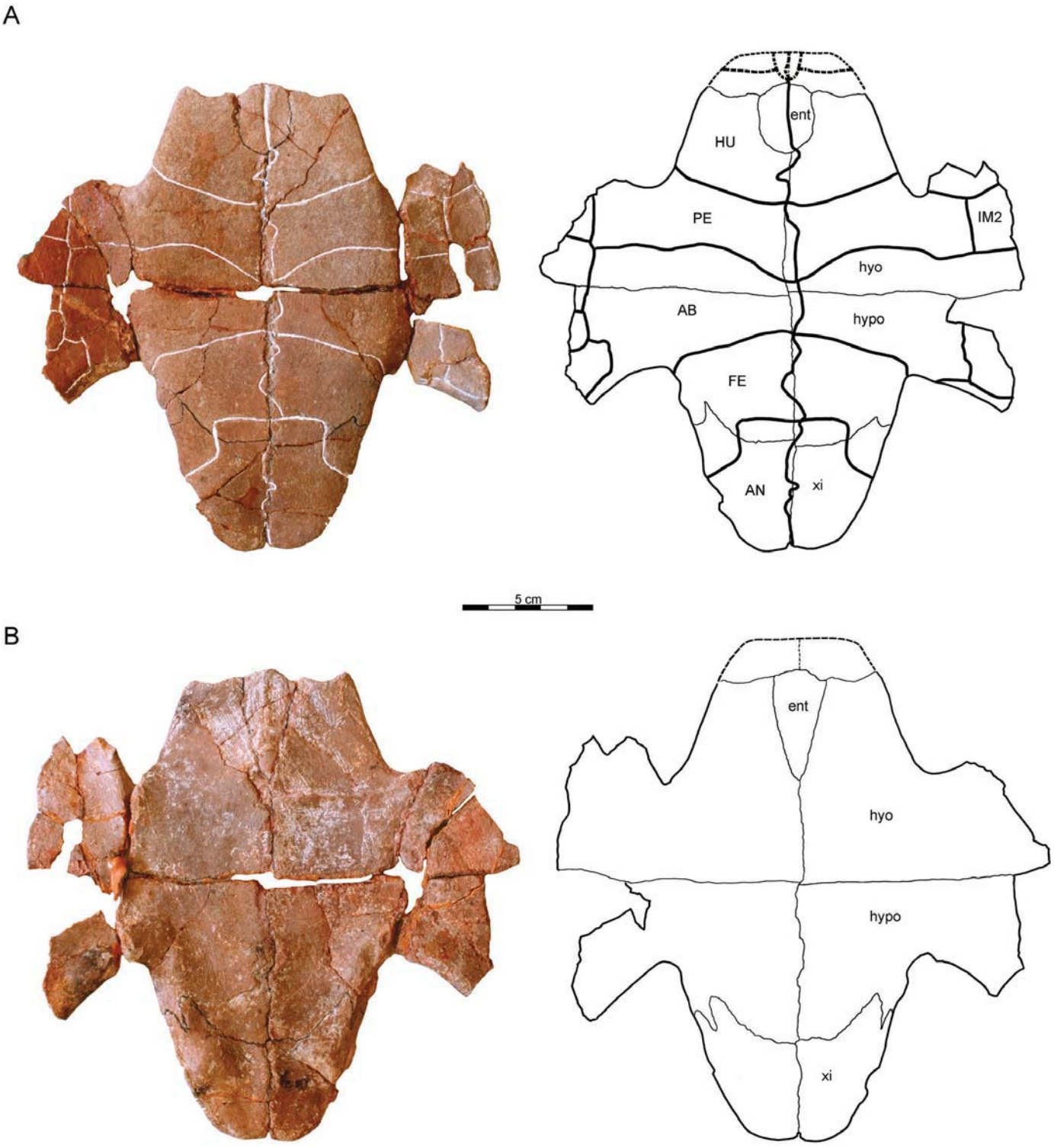

FIGURE 8. PIN 4636-5-1 (holotype), *Annemys latiens*, plastron, Late Jurassic, Shar Teg, Ulan Malgait beds, Govi Altai Aimag, Mongolia. **A**, photograph and line drawing in ventral view; **B**, photograph and line drawing in dorsal view. **Abbreviations**: **AB**, abdominal; **AN**, anal; **ent**, entoplastron; **FE**, femoral; **HU**, humeral; **hyo**, hyoplastron; **hypo**, hypoplastron; **IM**, inframarginals; **PE**, pectoral; **xi**, xiphiplastron.

PIN 4636-7 is a partial shell associated with a humerus (Figs. 10, 12C). It agrees with the morphology of the type specimen of *A. latiens* in having a hexagonal neural 1, a quadrangular neural 2, elongated vertebrals 2 and 3, marginals 4–8 overlapping onto costals (also likely present in the type of *A. levensis*), and a shorter, wider posterior plastral lobe (Fig. 10B). However, unlike the type of *A. latiens*, this specimen has a complete series of neurals preventing the midline contact of both costals 7 and 8. As a consequence, neural 7 is a regular hexagonal element with short sides facing anteriorly versus the pentagonal shape seen in the

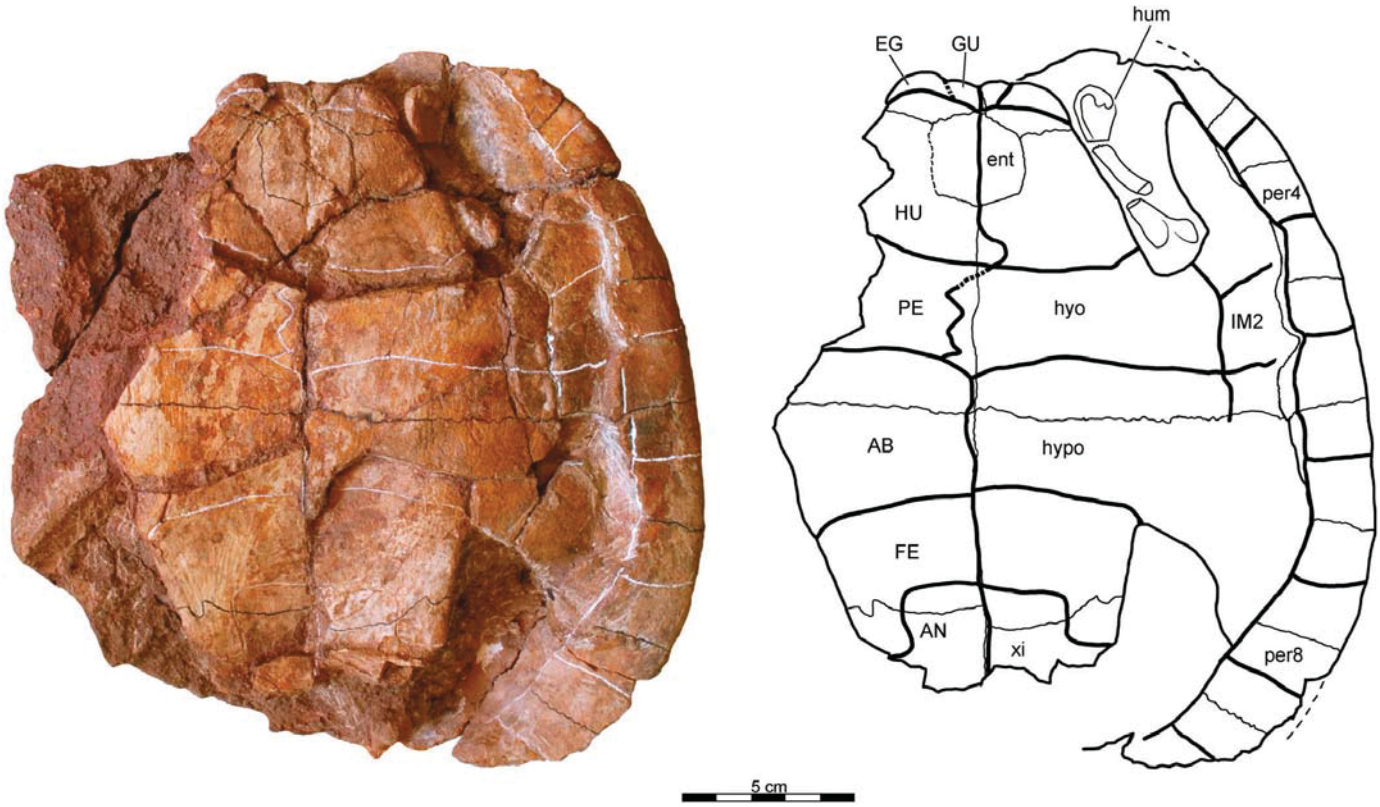

FIGURE 9. PIN 4636-6-2, *Annemys latiens*, plastron and incomplete carapace associated with the PIN 4636-6-2 skull, Late Jurassic, Shar Teg, Ulan Malgait beds, Govi Altai Aimag, Mongolia, photograph and line drawing of shell in ventral view. **Abbreviations**: **AB**, abdominal; **AN**, anal; **EG**, extragulars; **ent**, entoplastron; **FE**, femoral; **GU**, gular; **HU**, humeral; **hum**, humerus; **hyo**, hyoplastron; **hypo**, hypoplastron; **IM**, inframarginals; **PE**, pectoral; **per**, peripheral; **xi**, xiphiplastron.

holotype. Peripheral 1 has a wide contact with costal 1, unlike the holotype of *A. latiens*. A further difference is that in PIN 4636-7 the sulcus between vertebrals 3 and 4 crosses neural 5 instead of neural 6, but vertebrals 4 and 5 display an abnormal, asymmetric morphology and we therefore do not give this difference much weight (Fig. 10A). Plications of the vertebrals are more apparent in PIN 4636-7 than in the holotype of *A. latiens*.

DESCRIPTION OF *ANNEMYS* SP.

Hundreds of fragmentary turtle remains have been collected from the fossiliferous layers at Shar Teg, in particular isolated shell, girdle, and limb bones. Although some of these finds have been cataloged, the vast majority remains without numbers. Our study of the available material reveals that all fragments from Shar Teg originate from turtles of the same size class and that all fragments are consistent with the morphology seen in *Annemys levensis* and *A. latiens*, although species-level differences cannot be discerned. Although little is known about the morphology of coeval xinjiangchelyid turtles, and although the possibility must be acknowledged that some of these remains originate from other taxa, we herein refer all fragmentary material from Shar Teg to *Annemys* sp. and provide a description of the most important elements.

Peripherals

The peripherals (Fig. 11), particularly the bridge peripherals, are relatively thick compared with the small size of *Annemys levensis* and *A. latiens*. Peripheral 1 has a triangular outline and is rather thin and straight in cross-section. Its thickness, however, is 1.5 times greater posteriorly than anteriorly. Dorsally, its margin has an almost flat surface, whereas ventrally it is rounded. Some peripherals 1 are indistinctly guttered, but clear guttering is apparent in peripherals 2–7. The pleuromarginal sulcus passes close and parallel to the medial border of peripheral 1 and one specimen shows the sulcus coinciding with the peripheral 1/nuchal suture.

The posterior inner margin of the visceral side of peripheral 2 has a deep circular pit (or axillary fossa) for articulation with the anterior-most portion of the axillary buttress (Fig. 11A, B). This pit is partially confluent in some specimens with an additional, short, and finger-like scar that is situated at the sutural boundary between peripherals 2 and 3 and that serves as the insertion site for a peg of the hyoplastron (Fig. 11B): however, in other specimens these two structures are separated from one another (Fig. 11A). The position of the axillary fossa is variable ranging from the posterior fifth to the middle of peripheral 2, although it remains unclear whether these differences represent species characteristics. In cross-section, peripheral 2 has a subtriangular outline (Fig. 11A, B) and posteriorly it is two times thicker than anteriorly. The pleuromarginal sulcus passes slightly offset from the medial border of the plate and the intermarginal sulcus crosses the pleuralmarginal sulcus at the level of its anterior third.

Peripheral 3 (together with bridge peripherals 4–7) is elongated, 'C'-shaped in cross-section, and forms the anterior end of the bridge. The ventral plate of the medial rim bears two small pits that are aligned in a row for the reception of the pegs of the hyoplastron (Fig. 11C). The dorsomedial rim of peripherals 4–6

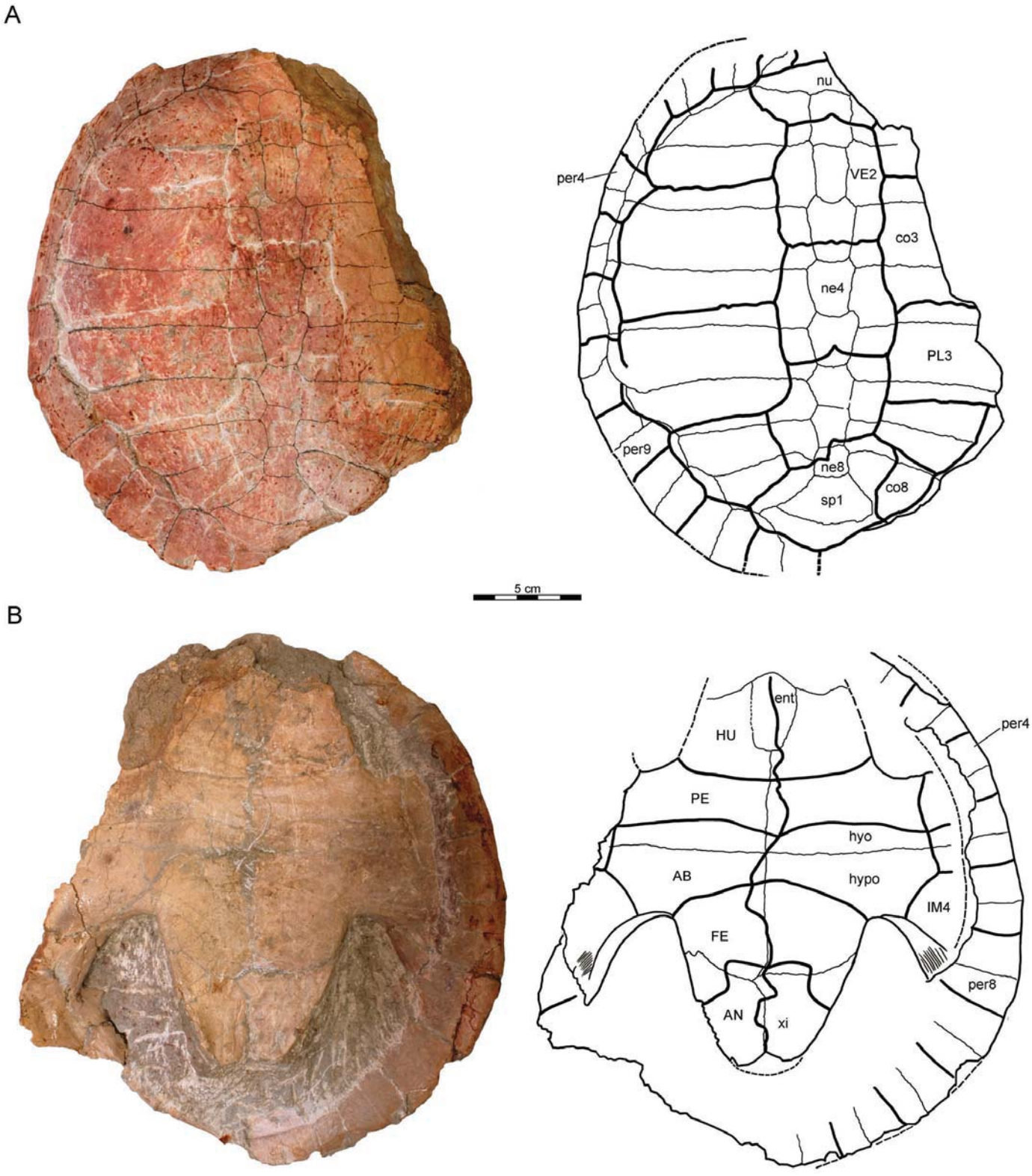

FIGURE 10. PIN 4636-7, *Annemys latiens*, shell, Late Jurassic, Shar Teg, Ulan Malgait beds, Govi Altai Aimag, Mongolia. **A**, photograph and line drawing of carapace in dorsal view; **B**, photograph and line drawing of plastron in ventral view. **Abbreviations**: **AB**, abdominal; **AN**, anal; **co**, costal; **ent**, entoplastron; **FE**, femoral; **HU**, humeral; **hyo**, hyoplastron; **hypo**, hypoplastron; **IM**, inframarginal; **ne**, neural; **nu**, nuchal; **PE**, pectoral; **per**, peripheral; **PL**, pleural; **sp**, suprapygal; **VE**, vertebral; **xi**, xiphiplastron.

(Fig. 11D–F) have a deep emargination where the corresponding convexity of the costal fits (Fig. 11D). These elements are more widely open than peripheral 3.

The medial edge of the ventral plate peripheral 7 (Fig. 11G, H) is perforated with a row of three shallow pits for the plastral pegs. Posteriorly, the pits are replaced by the anterior portion of the well-developed inguinal scar. Dorsal to and between the inguinal scar and the pits for the pegs, peripheral 7 received the free rib end of costal 5. Anteriorly, it is 'C'-shaped in cross-section, whereas posteriorly it is rather triangular and narrow.

Peripheral 8 is wider than long. The inguinal buttress terminates in a circular pit at the anterior inner corner (Fig. 11I). At the posterior inner corner, there is the pit for the insertion of the free rib of costal 6. In cross-section, peripheral 8 is half-moon-shaped (Fig. 11I).

Peripherals 9–11 are wide and flat, with gradually narrowing outline towards to lateral edge in cross-section. The free ribs insert anteriorly in peripheral 9, along the posterior half in 10 and approximately in the middle in 11.

Humerus

A humerus is associated with a shell that is referred to *Annemys latiens* (PIN 4636-7). The well-developed lateral process is placed at the same level as the humeral head and it is oriented ventrolaterally and therefore visible dorsally (Fig. 12C). A humeral shoulder is present. The medial process is slightly more reduced and rounded and the deltopectoral crest extends along the proximal fourth of the shaft. The humeral head is subspherical in dorsal view, with the anterior margin being narrower than the posterior. The shaft is relatively straight and more than twice long as wide. The ectepicondylar foramen is present in a form of a channel and not a fully open groove.

Femur

The femur has a subcircular femoral head and a slightly curved shaft (Fig. 12D). The femur is barely longer than the humerus. The trochanters are moderately developed. The proximal epiphysis has a similar width as the distal one. The trochanter minor faces anteriorly, the trochanter major faces dorsally, and the femoral head only slightly extends above the trochanters.

Scapula

The scapula lacks bony laminae between the dorsal process and the acromion, the glenoid and the acromion, and the glenoid and the dorsal process (Fig. 12B). A well-developed glenoid neck is present and the glenoid is sutured. The relative proportions of the scapular processes show that the acromion is more than half the length of the dorsal process and the angle between them is slightly more than 90°.

Pelvis

Apart from numerous isolated pelvic elements, an excellent complete pelvis comes from the Shar Teg locality (Fig. 12A). The pelvis is well ossified and it was ligamentously attached to the shell. The thyroid fenestrae are separated by a midline projection formed by the pubes and the ischia. The lateral pubic process is well developed, flat, and faces ventrolaterally, and the lateral ischial process is roughly as long as the metischial process. The posterior ilial process is almost perpendicular to the iliac neck in lateral view. The ilium has an elongated neck and a thelial process is absent. The acetabulum is not fused and lacks a posterior notch.

PHYLOGENETIC ANALYSIS

Methods

A maximum parsimony analysis was performed using TNT (Goloboff et al., 2008) based on the character-taxon matrix of Sterli and de la Fuente (2013), which in return is based on that of Joyce (2007), Sterli and de la Fuente (2011), and Sterli et al. (2013). The matrix was expanded by adding five taxa in particular: *Xinjiangchelys radiplicatoides*, *X. junggarensis* (sensu Brinkman et al., 2008), *Annemys levensis*, *A. latiens*, and *Basilochelys macrobios* Tong, Claude, Naksri, Suteethorn, Buffetaut, Khansubha, Wongko, and Yuangdetkla, 2009. The scorings of *X. radiplicatoides* are based on Brinkman et al. (2013), those of *X. junggarensis* on personal observation of IVPP material from Pingfengshan described in Peng and Brinkman (1993), those of *A. levensis* and *A. latiens* based on personal observation of PIN material, and those of *B. macrobios* based on Tong et al. (2009) and photographs obtained from H. Tong. We refrained from adding poorly known/described relevant taxa (e.g., *Anatolemys* spp., *Shartegemys laticentralis*, *Macrobaena mongolica*) to the matrix to minimize the risk of introducing mistakes.

We note that the scorings for *Xinjiangchelys latimarginalis* sensu Peng and Brinkman (1993) (= *X. junggarensis* sensu Brinkman et al., 2008) are likely based on a chimera. Brinkman and Wu (1999) used *X. latimarginalis* as a terminal taxon, but their scorings were based on material from two distantly placed localities: the shell characters were based on material from the Pingfengshan locality of the Junggar Basin, Xinjiang, China (Peng and Brinkman, 1993), whereas the skull characters were scored for material from Kyrgyzstan (Fergana Basin, Sarykamyshsay locality) after Kaznyshkin et al. (1990). However, Nessov (1995) separated the Fergana *X. latimarginalis* from the Junggar *X. latimarginalis* and included the former into a new species, *X. tianshanensis*. Joyce (2007) and all subsequent phylogenetic workers adopted the scorings of Brinkman and Wu (1999) for *X. latimarginalis*. For the present analyses, we considered *X. latimarginalis* synonymous with *X. junggarensis*, as suggested by Brinkman et al. (2008), and rescored this taxon based on Pingfengshan material only, as observed directly by W.G.J. and M.R. or described in Peng and Brinkman (1993). All skull characters for this taxon were therefore scored as '?' because no skull material is available from this locality.

The following scorings were changed relative to the matrix of Sterli and de la Fuente (2013; original scorings of Sterli and de la Fuente are in parenthesis): Epiplastron B: *Hangaiemys hoburensis*: 1 (?), *Sinemys lens* 1 (?); Pterygoid B: *Hangaiemys hoburensis* 1(2), *Dracochelys bicuspis* 1(2), *Pleurosternon bullockii* 1(2), *Kallokibotion bajazidi* 1(2), *Mongolochelys efremovi* 1(2), *Peligrochelys walshae* 1(2), *Chubutemys copelloi* 1(2) *Niolamia argentina* Ameghino, 1899?(2), *Eileanchelys waldmani* ?(2); Carapace D: *Hangaiemys hoburensis* 0(?), *Chengyuchelys baenoides* Young and Chow, 1953 (IVPP-V6507) 0(1); Carapace E: *Hangaiemys hoburensis* –(?); Vertebral A: *Siamochelys peninsularis* ?(1); Vertebral C: *Siamochelys peninsularis* ?(1); Anal A: *Siamochelys peninsularis* ?(0), *Chengyuchelys baenoides* ?(0); Entoplastron B: *Chengyuchelys baenoides* ?(1); Mesoplastron A: *Siamochelys peninsularis* 2(0); Hypoplastron A: *Chengyuchelys baenoides* ?(0); Xiphiplastrons A and B: *Chengyuchelys baenoides* ?(0); Dorsal Rib A: *Siamochelys peninsularis* ?(2); Plastral Scute B: *Siamochelys peninsularis* Tong, Buffetaut, and Suteethorn, 2002: 1(0).

The character Cervical Vertebrae A was omitted from the analysis because we found it difficult to replicate this character objectively and perceived a number of inconsistencies in the matrix. The character Diploid Number A was also omitted following the discussion in Joyce and Bell (2004) and Joyce (2007).

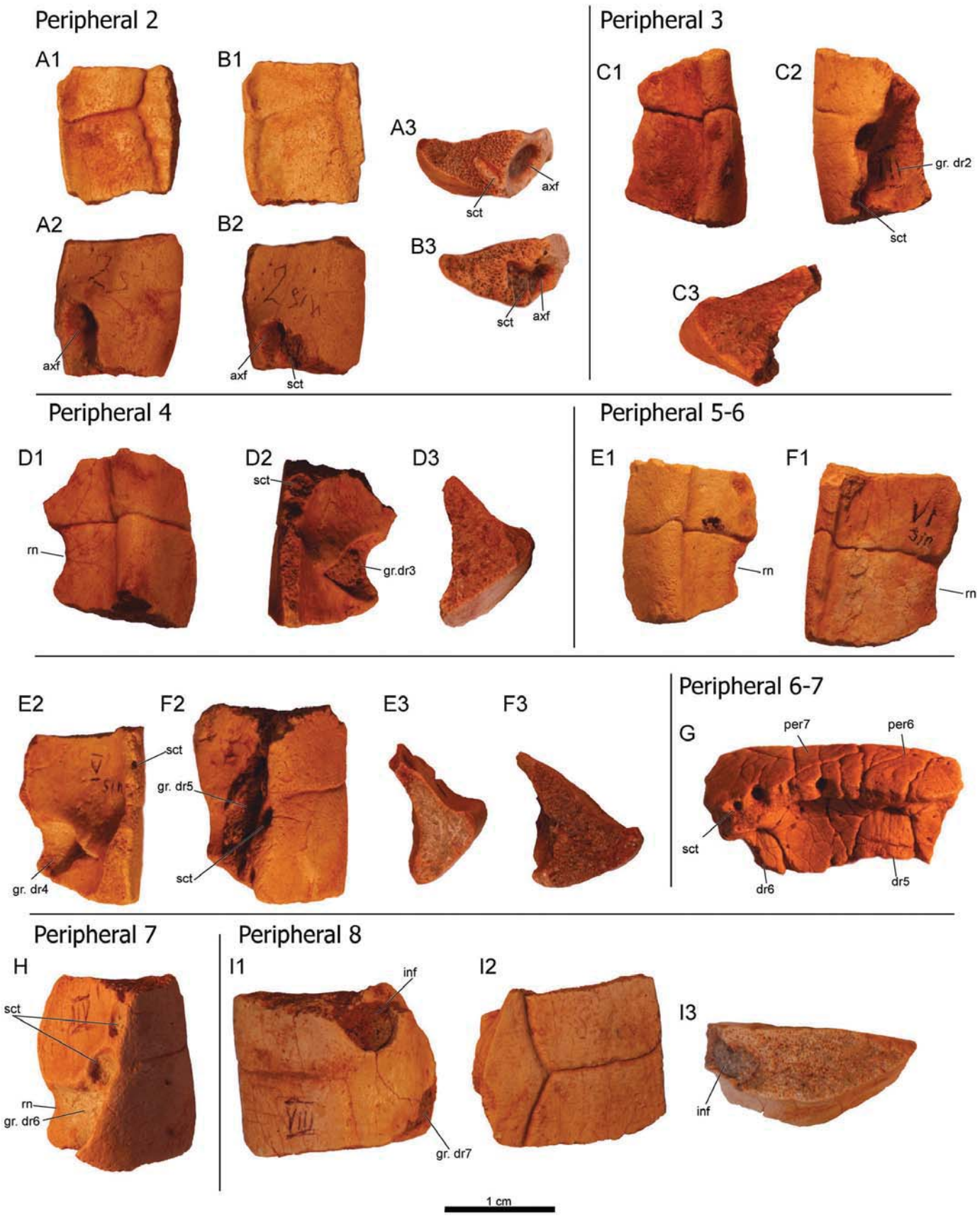

The following characters were treated as ordered: 7 (Nasal A), 19 (Parietal H), 27 (Squamosal C), 40 (Maxilla D), 42 (Vomer A), 50 (Quadrate B+C), 52 (Antrum Postoticum A), 59 (Pterygoid B), 81 (Opisthotic C), 82 (Opisthotic D), 89 (Stapedial Artery B), 98 (Canalis Caroticum F), 120 (Carapace A), 121 (Carapace B), 130 (Peripheral A), 133 (Costal B), 138 (Supramarginal A), 158 (Hyoplastron B), 159 (Mesoplastron A), 161 (Hyoplastron B), 176 (Abdominal A), 213 (Cleithrum A), 214 (Scapula A), 232 (Manus B), and 233 (Manus C). *Sphenodon punctatus*, *Owenetta kitchingorum*, *Simosaurus gaillardoti*, and *Anthodon serrarius* were designated as outgroups following Sterli and de la Fuente (2013).

A preliminary analysis of this character-taxon matrix failed in that multiple runs consistently arrived at different results. We suspect that these difficulties are caused by a combination of rampant homoplasy, missing data, and the sheer size of the matrix. Given that this analysis is focused on the phylogenetic relationships and placement of xinjiangchelyid turtles, we decided to crop taxa not pertinent to these questions (e.g., most derived baenids, most meiolaniiforms) and a broad spectrum of taxa known from fragmentary material only (see Appendix 1 for a complete list). The resulting matrix consists of 237 characters for a total of 83 terminal taxa. The character-taxon matrix and the TNT file are provided as Supplementary Data.

The most parsimonious trees were found using two rounds of the heuristic search tree-bisection-reconnection (TBR), during which thousands of random addition sequences replicates were produced and 15 trees saved per replicate. The trees retained in the memory were exposed to a second round of TBR. The relationships of living cryptodiran taxa were manually constrained according to recent results of molecular phylogenetic studies (as suggested by Danilov and Parham, 2006, 2008), without assuming a priori, however, that Trionychia nests within Cryptodira (Krenz et al., 2005; Barley et al., 2010). The internal relationships of durocryptodires were constrained using the molecular topology of Barley et al. (2010) (i.e., (Emydidae (Geoemydidae + Testudinidae)) + (Chelonioidea (Chelydridae + Kinosternoidea)))). The complete list of taxa designated as floaters can be found in Appendix 2. By enforcing these constraints, TNT failed to find the most parsimonious trees (MPTs); therefore, the heuristic search was repeated until the MPTs were found 30 times during each replicate (using the command 'xmult = hits 30;'). After this, the trees retained in the memory were exposed to a second round of TBR. Strict consensus trees were calculated and rogue taxa were pruned a posteriori from the constrained analyses to achieve better resolution.

Results

The second round of TBR found 2916 trees (length = 867 steps) with a poorly resolved strict consensus topology. Nevertheless, an unresolved xinjiangchelyid clade composed of *Annemys levensis*, *A. latiens*, *Xinjiangchelys radiplicatoides*, and *X. junggarensis* was recovered, supported by a single unambiguous synapomorphy: presence of pronounced sinusoidal midline plastral sulcus (Plastral Scutes B). This clade has an unorthodox placement outside of crown group Testudines in a polytomy with baenids and pleurosternids (Fig. 13; see also Supplementary Data, Fig. S1, for complete consensus tree). When *X. junggarensis* is pruned (not shown), *A. levensis* is found as the sister taxon of *X. radiplicatoides* and *A. latiens*. Several wildcard taxa are identified, including *Yehguia tatsuensis*, *Basilochelys macrobios*, *Adocus beatus*, *Shachemys laosiana*, *Plesiochelys etalloni*, *Solnhofia parsonsi*, *Portlandemys mcdowelli*, *Santanachelys gaffneyi*, '*Thalassemys*' *moseri*, *Xinjiangchelys junggarensis*, *Siamochelys peninsularis*, *Chengyuchelys baenoides*, and *Judithemys sukhanovi*. When these taxa are pruned from the consensus cladogram (not shown), *Ordosemys leios*, *Dracochelys bicuspis*, *Sinemys lens*, and *Hangaiemys hoburensis* are placed at the stem of Testudines.

Following our proposed definitions, Xinjiangchelyidae consists of *A. levensis*, *A. latiens*, *X. radiplicatoides*, and *X. junggarensis*, whereas Sinemydidae only consists of *S. lens*. The name Macrobaenidae cannot be applied because it is not included in our analysis.

DISCUSSION

Phylogenetic Relationships of Xinjiangchelyidae

Our analysis clearly recovered a monophyletic clade that partially recreates the 'traditional' concept of Xinjiangchelyidae of some authors (e.g., Sukhanov, 2000) and to which the phylogenetic definition of the name Xinjiangchelyidae applies. The position of Xinjiangchelyidae outside of Testudines is, on the other hand, a rather unorthodox result (Fig. 13). Xinjiangchelyids are known to possess several primitive characters, including the presence of nasals, amphicoelous cervical vertebrae, chevrons, and dorsal process of epiplastron, yet previous analyses hypothesized a more derived position within Pancryptodira (Brinkman and Wu, 1999; Gaffney et al., 2007; Joyce, 2007; Danilov and Parham, 2008; Tong et al., 2009, 2012a; Anquetin, 2012) or near the base of crown Testudines (Sterli, 2010; Sterli and de la Fuente, 2011). The basal position in the present analysis is likely caused by numerous changes we undertook to the scoring of *Xinjiangchelys junggarensis*, *Siamochelys peninsularis*, and of *Annemys* from Shar Teg, which almost universally resulted in the recognition of primitive character states in these taxa (e.g., presence of interpterygoid vacuity, presence of basipterygoid process, open foramen jugulare posterius, long dorsal rib 1, position of the transverse process of the cervical in the middle of the centrum). Given that we are aware of similar adjustments to the scoring that will need to be undertaken for various sinemydids, macrobaenids, and plesiochelyids, we consider our results tentative pending a revision of the detailed morphology of the aforementioned taxa.

The results of our analysis are partially consistent with the only previous global analysis that included *Annemys levensis* (Anquetin, 2012), who scored this taxon on the basis of the preliminary reports by Sukhanov (2000) and Sukhanov and Narmandakh (2006). The analysis of Anquetin (2012) recovered Xinjiangchelyidae within Testudines and revealed that it consists of five taxa, including *Xinjiangchelys qiguensis*, *X. latimarginalis* sensu Peng and Brinkman, 1993 (= *X. junggarensis*), *X. tianshanensis*, *Annemys levensis*, and *Siamochelys peninsularis*. Although our analyses differs in the position of

← FIGURE 11. *Annemys* sp., peripherals, Late Jurassic, Shar Teg, Ulan Malgait beds, Govi Altai Aimag, Mongolia. **A**, PIN 4636-15, left peripheral 2, **A1**, dorsal view, **A2**, ventral view, **A3**, posterior view; **B**, PIN 4636-22, left peripheral 2, **B1**, dorsal view, **B2**, ventral view, **B3**, posterior view; **C**, PIN 4636-17, peripheral 3, **C1**, dorsal view, **C2**, ventral view, **C3**, anterior view; **D**, PIN 4636-23, right peripheral 4, **D1**, dorsal view, **D2**, ventral view, **D3**, posterior view; **E**, PIN 4636-18, left peripheral 5, **E1**, dorsal view, **E2**, ventral view, **E3**, anterior view; **F**, PIN 4636-19, left peripheral 6, **F1**, dorsal view, **F2**, ventral view, **F3**, anterior view; **G**, PIN 4636-16, right incomplete peripheral 6 and peripheral 7, ventral view; **H**, PIN 4636-20, left peripheral 7, ventral view; **I**, PIN 4636-21, left peripheral 8, **I1**, ventral view, **I2**, dorsal view, **I3**, anterior view. **Abbreviations**: **axf**, axillary fossa; **gr. dr**, groove for reception of tip of dorsal rib; **inf**, inguinal fossa; **per**, peripheral; **rn**, rib notch; **sct**, socket for plastral peg.

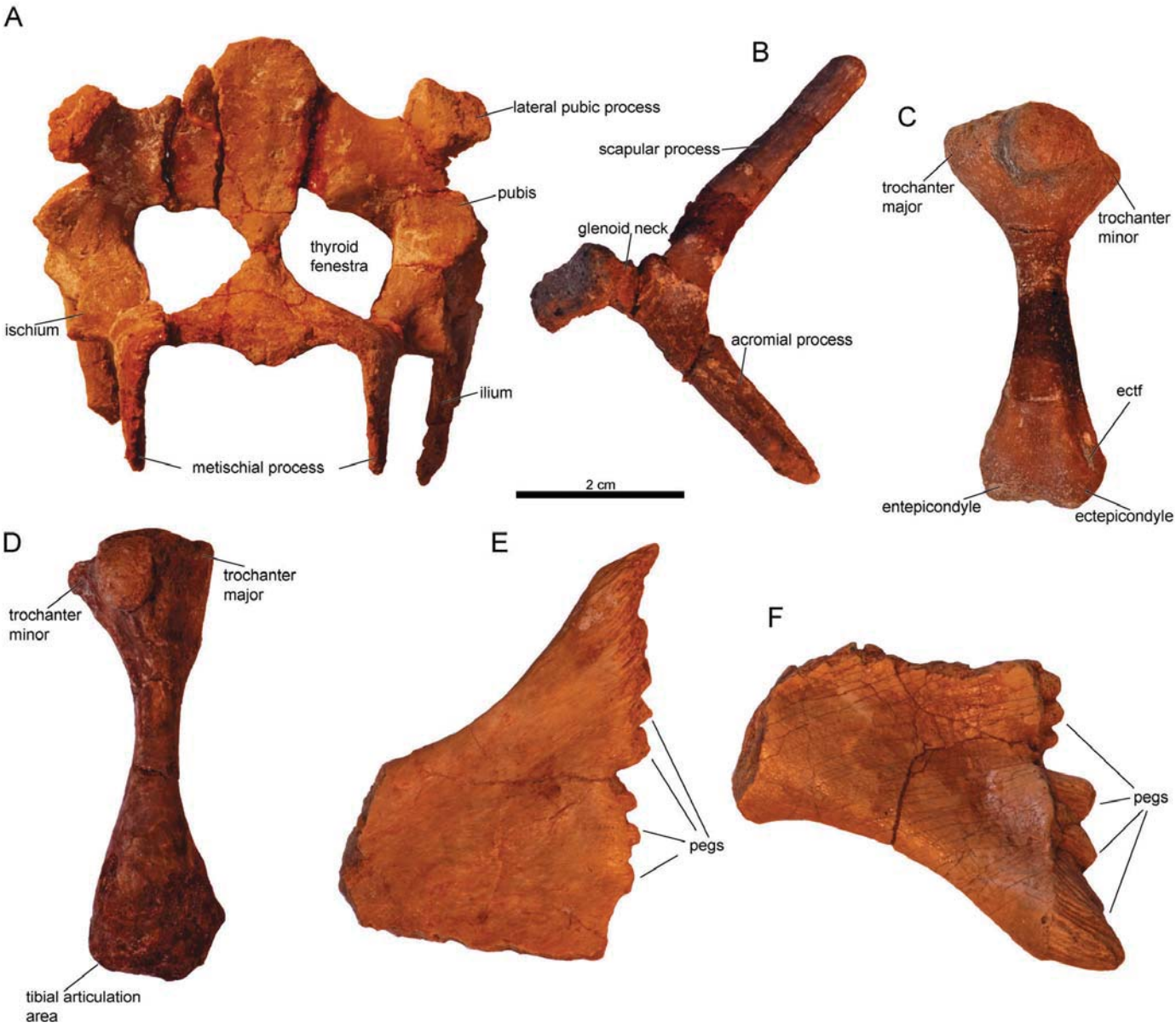

FIGURE 12. *Annemys* sp., appendicular elements, Late Jurassic, Shar Teg, Ulan Malgait beds, Govi Altai Aimag, Mongolia. **A**, PIN 4636-10, *Annemys* sp. pelvis in ventral view; **B**, PIN 4636-11, *Annemys* sp. right scapula in lateral view; **C**, PIN 4636-7, *A. latiens* right humerus in dorsal view; **D**, PIN 4636-12, right femur in dorsal view; **E**, PIN 4636-13, *Annemys* sp. left lateral part of hyoplastron with axillary buttress in ventral view; **F**, PIN 4636-14, *Annemys* sp. right lateral part of hypoplastron with inguinal buttress in dorsal view. **Abbreviation**: **ectf**, ectepicondylar foramen.

Xinjiangchelyidae and *Siamochelys peninsularis*, our study agrees with Anquetin (2012) in that *A. levensis* and *X. junggarensis* (= *X. latimarginalis*) are members of the group in question.

Presence of a Reduced Interpterygoid Vacuity in *Annemys*

One of the most interesting observations regarding the cranial morphology of *Annemys levensis* and *A. latiens* is the presence of a small gap between the pterygoid and the basisphenoid. In basal turtles, such as *Proganochelys quenstedti* Baur, 1887, *Kayentachelys aprix* Gaffney, Hutchison, Jenkins, and Meeker, 1987, and *Condorchelys antiqua* Sterli, 2008, the palatine artery entered the skull via a wide gap between the pterygoids, the interpterygoid vacuity. The vacuity is absent in all more derived fossil turtles and the palatine artery therefore entered the skull through a pair of distinct foramina, the foramina posterius canalis carotici lateralis (fpccl). *Annemys latiens* clearly displays an intermediate morphology by displaying both a pair of fpccl and remnants of the pterygoid vacuity. The corresponding region in *A. levensis* is somewhat damaged, but a pair of grooves that lead to the lateral edge of the gap and that evidently held the palatine arteries is indicative of the former presence of paired fpccl. Slit-like fpccl have otherwise been reported for *Xinjiangchelys radiplicatoides* (Brinkman et al., 2013), but this taxon shows no sign of a gap anterior to the basisphenoid and therefore represents the derived condition. The slit-like shape of the palatine foramina implies that the anterior contact of the basisphenoid with the pterygoid was at best poorly ossified in this xinjiangchelyid. An unossified area between the pterygoids coupled with fpccl is also present in *Annemys* sp. from Wucaiwan, Junggar Basin

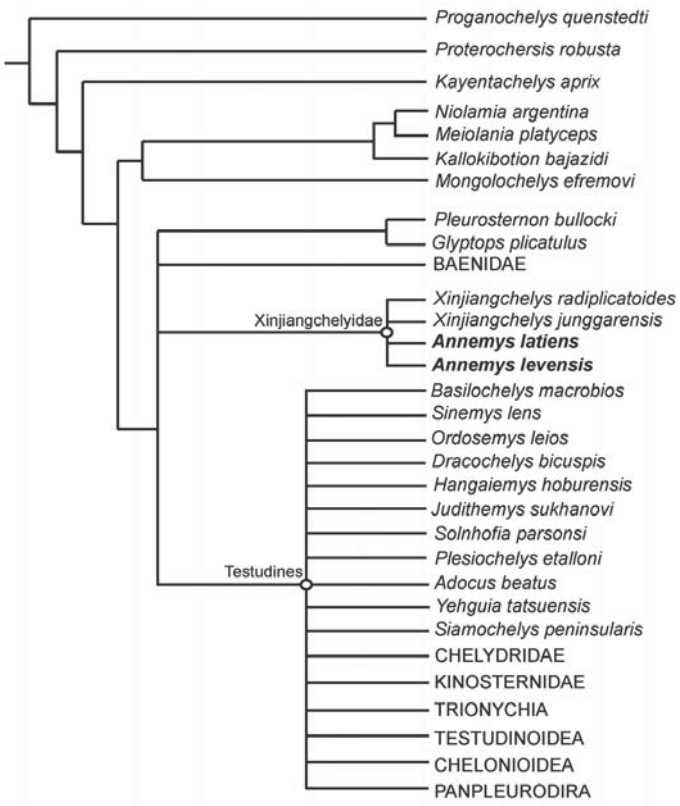

FIGURE 13. Simplified strict consensus tree of 2916 equally parsimonious trees (length = 867 steps) obtained after a maximum parsimony analysis of the modified taxon-character matrix of Sterli and de la Fuente (2013) including 83 taxa and 237 characters. The internal relationships of Durocryptodira is constrained after Barley et al. (2010): (Emydidae (Geoemydidae + Testudinidae)) + (Chelonioidea (Chelydridae + Kinosternoidea))). The inclusion of *Annemys latiens*, *A. levensis*, and *Xinjiangchelys radiplicatoides* into Xinjiangchelyidae is only supported by one character: presence of pronounced midline plastral sulcus (Plastral Scutes B). For complete consensus tree, see Supplementary Data, Figure S1.

(Brinkman et al., 2013), and is therefore consistent with the morphology of *A. latiens* and what is inferred for A. *levensis*. A larger sample of xinjiangchelyid skulls may eventually reveal that the gap between the pterygoids closes during ontogeny and abundant material from the Turpan Basin (Wings et al., 2012) is particularly promising (pers. observ. of material by M.R. and W.G.J.).

The palatine arteries probably entered via the fpccl in these taxa and the xinjiangchelyid condition may represent an evolutionary stage when the interpterygoid vacuity was not yet closed completely but already lost its function in carrying the palatine artery.

Taxonomy of *Annemys*

The taxa *Annemys levensis* and *A. latiens* were used informally in Sukhanov (2000) for material from the Upper Jurassic of Shar Teg, Mongolia, and the names were only made available following the rules of the International Commission on Zoological Nomenclature in a subsequent paper by Sukhanov and Narmandakh (2006). *Annemys latiens* is based on an almost complete shell (PIN 4635-5-1) associated with a poorly preserved lower jaw ramus and multiple skull fragments, of which the partial basicranium (PIN 4635-5-2) is the most informative. This damaged skull was not reported in Sukhanov (2000) or Sukhanov and Narmandakh (2006) and *A. latiens* was diagnosed relative to *A. levensis* on the basis of shell characters only (Sukhanov and Narmandakh, 2006). Another, previously unreported *A. latiens* skull-shell association from Shar Teg (PIN 4636-6) reveals distinct cranial differences relative to the skull of *A. levensis* (see above) and thereby supports the presence of two separate taxa at Shar Teg using cranial characters. The carapace (PIN 4636-6) of the associated skull is very incomplete, but its wide posterior plastral lobe is consistent with the morphology seen in the holotype of *A. latiens*. The small amount of information that we were able to extract from the badly preserved holotype skull of *A. latiens* (PIN 4636-5-2) agrees with PIN 4636-6-2 in being narrow and elongated, unlike *A. levensis* (see the description of PIN 4636-6-2 above). We tentatively also refer another shell (PIN 4636-7) to *A. latiens* based on the proportions of the posterior plastral lobe (see the description of this shell above). *Annemys levensis* is therefore only known from a single specimen, the type specimen (PIN 4636-4), which consists of an associated skull, lower jaw, shell, and some other appendicular elements. Additional material from Shar Teg may allow a better understanding of the intra- and interspecific variation in *Annemys* and at present it seems difficult to distinguish the two species on the basis of discrete shell characters. The lack of characters that allow distinguishing the postcranial of *A. levensis* and *A. latiens* forces us to refer all fragmentary remains to *Annemys* sp.

Matzke et al. (2004b) and Tong et al. (2012b) both synonymized *Annemys* with *Xinjiangchelys* because their phylogenetic analysis of 'xinjiangchelyids' revealed *A. levensis* and *A. latiens* to be situated within a clade formed by taxa typically attributed to *Xinjiangchelys*. However, neither analysis included any member of the 'sinemydid-macrobaenid' grade or other more advanced Pancryptodires but instead extensively sampled 'xinjiangchelyid' taxa—to an extent that it seems the authors a priori inferred that *Annemys* belong to the latter group. Our global analysis found *Annemys levensis* in a monophyletic clade with *X. latimarginalis* (sensu Peng and Brinkman, 1993), but the inclusion of more xinjiangchelyid taxa are required to test the monophyly of this group and the relationship of *Annemys* to *Xinjiangchelys* spp. Our analysis found no evidence for the exclusive monophyly of *Annemys* (Fig. 13), but we do not consider our analysis to be a highly rigorous test of the relationships of this taxon within xinjiangchelyids because our taxonomic sample is limited for this group. Until the phylogenetic relationships of xinjiangchelyid taxa have been resolved with greater assurance, we suggest keeping the name *Annemys*.

Brinkman et al. (2013) recently described and figured a skull with associated shell elements from the Upper Jurassic of the Junggar Basin (Wucaiwan area, Xinjiang, China) that they referred to *Annemys* sp. (also figured in Rabi et al., 2010:fig. 1g, h). As in A. *latiens* and A. *levensis*, this skull has an unossified gap anterior to the basisphenoid between the pterygoids; therefore, we agree that it is morphologically closer to *Annemys* spp. than to *Xinjiangchelys radiplicatoides*. We also agree that this skull is clearly different from that of *A. levensis* (see Brinkman et al., 2013, for a list of differences). The *Annemys* sp. skull is furthermore different from *A. latiens* in its proportions, by being less elongated and by having a distinctly more extensive frontal and jugal contribution to the orbit compared with *A. latiens*. We therefore suggest that this fossil represents a taxon different from both *A. levensis* and *A. latiens*, but likely closely related to them.

Paleoecology of *Annemys*

The overall shell morphology and the size of *A. latiens* and *A. levensis* are highly similar and these taxa are therefore only poorly diagnosed by the shells. On the other hand, the skulls of these two turtles are greatly different in the arrangement of the

dermal roofing elements and in their relative proportions: *A. latiens* has an elongated and narrow skull compared with the relatively broad skull of *A. levensis*.

Both species originate from a single larger horizon at Shar Teg (i.e., the Ulan Malgait beds); therefore, they may have been sympatric taxa, although no clear record exists of their co-occurrence in identical layers. However, whereas the absence of size difference may have allowed both taxa to share the same aquatic habitat, the distinct skull shapes suggest niche partitioning in terms of feeding strategies.

It is apparent from the depositional environment in which they were found that *Annemys latiens* and *A. levensis* were freshwater turtles. This conclusion is further supported by their overall anatomy: low, suboval shell, flat skull, and relatively straight humeral and femoral shafts. However, these two taxa were probably not as adapted to the aquatic realm as *Hangaiemys* (*Kirgizemys*) *hoburensis*, *Ordosemys leios*, or *Sinemys lens*, all of which exhibit more reduced shells. The flat, triangular skull with narrow and sharp triturating surfaces in *Annemys* spp. is consistent with a predatory lifestyle. In being elongated and flat, *A. latiens* had an even more streamlined skull compared with *A. levensis,* which may have been of great help while striking at small agile prey such as fish. Future collecting at Shar Teg should focus on finding the cervical vertebrae of *Annemys* in order to clarify whether they were short- or long-necked forms.

The Ecological Diversity of Xinjiangchelyidae during the Late Jurassic—Xinjiangchelyids have so far been mostly known from their shells, which are surprisingly uniform and conservative in their morphology, although size differences of some taxa with uncertain affinities are apparent (e.g., Matzke et al., 2005). However, new data (Brinkman et al., 2013, and this paper) indicate that the skull shape of xinjiangchelyids was more variable than their shells. At present, only a few xinjiangchelyids are known from their skulls, but these can nevertheless be clearly classified into three morphotypes. The first morphotype is represented by an inflated and relatively high skull shape with shallow upper temporal emargination, as seen in *Xinjiangchelys radiplicatoides* (Brinkman et al., 2013). The second is small, flat, and triangular with deeper temporal emargination, as seen in *Annemys levensis* and *Annemys* sp. from the Junggar Basin (Brinkman et al., 2013). The third is an elongated, narrow variant of the second type and seen in *A. latiens*. These morphotypes probably correspond to different feeding niches and strategies and indicate that by the Late Jurassic, the dominant turtle clade of Asia achieved only a moderate level of ecological diversity relative to what is present in later (e.g. Cretaceous) Pancryptodires, a group in which xinjiangchelyids are traditionally placed. However, it must be noted that the lack of skull material for most Jurassic Asian turtles may result in a significant underestimate of their actual ecological diversity.

Functional Aspects of the Trochlear System in *Annemys*— The skulls of *A. latiens* and *A. levensis* reveal that the processus trochlearis oticum is very poorly developed in these taxa and may not even qualify as a real process. The trochlear structure is best preserved in the skull of *A. levensis*. It consists of a rugose area on the anterodorsal wall of the otic chamber (Fig. 1A, B) and lacks the protrusion seen in many crown cryptodires (e.g., Gaffney, 1979; Joyce, 2007; Sterli and de la Fuente, 2010; Joyce and Sterli, 2012). It is likely that this surface held the cartilage that redirected the temporal musculature (the cartilago transiliens) over the otic capsule before reaching the coronoid process of the lower jaw (Schumacher, 1973). The undeveloped bony base of the synovial capsule suggests that the trochlear system of *Annemys* was not as advanced as in crown cryptodires. This would be consistent with the thickened laterally protruding lip of the epipterygoid present in *A. levensis* that could have served as a barrier that hindered the adductor musculature from crossing the path of the trigeminal nerve. The primitive trochlear system of *Annemys* spp. could result in lower bite performance relative to most crown cryptodires. This is probably correlated with the short supraoccipital process (at least present in *A. levensis*) that only allows for a reduced amount of muscle mass, but also does not require an advanced and well-developed trochlear system (Herrel et al., 2002; Sterli and de la Fuente, 2010).

CONCLUSIONS

Our thorough morphological revision of all available material from the Late Jurassic locality of Shar Teg, Mongolia, confirms the presence of two species of *Annemys*, *A. latiens* and *A. levensis*. Although both species exhibit highly similar shells, they clearly differ in the morphology of their skulls. In particular, whereas *A. levensis* has the relatively broad skull typical of generalist aquatic feeders, *A. latiens* has the elongate skull typical of piscivorous turtles. It is therefore likely that these two turtles shared the same habitat but pursued distinct feeding strategies. We expect future collecting at Shar Teg to produce higher quality postcranial material and anticipate that these two taxa will be distinguishable based on shell characters at some point in the future.

Our inclusion of *A. latiens, A. levensis*, *Xinjiangchelys junggarensis*, and *X. radiplicatoides* into a global analysis of turtle relationships united these taxa in a weakly supported clade and resulted in the hypothesis that xinjiangchelyid turtles are derived stem turtles. This unorthodox result is the result of a number of unambiguously primitive characters that are present in xinjiangchelyid turtles, such as well-developed basipterygoid processes and remnants of the interpterygoid vacuity. A basal position of Middle–Late Jurassic xinjiangchelyid turtles is furthermore consistent with the expected time of origin of crown-clade Testudines (Joyce et al., 2013). We are nevertheless aware of significant inconsistencies that exist in the character-taxon matrix we used that have arisen from recent insights into the morphology of various other Asian Mesozoic turtles. We therefore anticipate that our results are preliminary and will be adjusted by future changes to this dynamic character-taxon matrix.

ACKNOWLEDGMENTS

We thank E. Syromyatnikova for patiently assisting M.R. and W.G.J. during their stay at PIN. D. Brinkman, T. Lyson, and J. Parham are thanked for insightful discussions. J. Sterli, D. Brinkman, and an anonymous reviewer provided valuable comments that helped improve the quality of the manuscript. J. Sterli is particularly thanked for her assistance in using TNT. This research was supported by Deutsche Forschungsgemeinschaft (DFG) grant JO 928/2-1 to W.G.J. The participation of I.D. in this study was supported by DFG grant MA 1643/14-1 and the Russian Foundation for Basic Research (project 11-04-91331-NNIO). M.R. was also supported by the MTA Lendület Program Project No. 95104.

LITERATURE CITED

Ameghino, F. 1899. Sinopsis geológica paleontológica. Suplemento (adiciones y correcciones). Censo Nacional, La Plata:1–13.

Anquetin, J. 2012. Reassessment of the phylogenetic interrelationships of basal turtles (Testudinata). Journal of Systematic Paleontology 10:3–45.

Barley, A. J., P. Q. Spinks, R. C. Thomson, and H. B. Shaffer. 2010. Fourteen nuclear genes provide phylogenetic resolution for difficult nodes in the turtle tree of life. Molecular Phylogenetics and Evolution 55:1189–1194.

Batsch, A. J. G. C. 1788. Versuch einer Anleitung, zur Kenntniß und Geschichte der Thiere und Mineralien. Akademische Buchhandlung, Jena, 528 pp.

Baur, G. 1887. Osteologische Notizen über Reptilien (Fortsetzung II). Zoologischer Anzeiger 10:241–268.

Bohlin, B. 1953. Fossil reptiles from Mongolia and Kansu. Report from the scientific expedition to the north and western provinces of China under the leadership of Sven Hedin. The Sino-Swedish Expedition VI—Vertebrate Palaeontology 6:1–113.

Brinkman, D. B. 2001. New material of *Dracochelys* (Eucryptodira: Sinemydidae) from the Junggar Basin, Xinjiang, People's Republic of China. Canadian Journal of Earth Sciences 38:1645–1651.

Brinkman, D. B., and J.-H. Peng. 1993a. New material of *Sinemys* (Testudines, Sinemydidae) from the Early Cretaceous of China. Canadian Journal of Earth Sciences 30:2139–2152.

Brinkman, D. B., and J.-H. Peng. 1993b. *Ordosemys leios*, n. gen., n. sp., a new turtle from the Early Cretaceous of the Ordos Basin, Inner Mongolia. Canadian Journal of Earth Sciences 30:2128–2138.

Brinkman, D. B., and X.-C. Wu. 1999. The skull of *Ordosemys*, an Early Cretaceous turtle from Inner Mongolia, People's Republic of China, and the interrelationships of Eucryptodira (Chelonia, Cryptodira). Paludicola 2:134–147.

Brinkman, D. B., J.-L. Li, and X.-K. Ye. 2008. Order Testudines; pp. 35–102 in J.-L. Li, X.-C. Wu, and F.-C. Zhang (eds.), The Chinese Fossil Reptiles and Their Kin. Science Press, Beijing.

Brinkman, D. B., D. Eberth, J. Clark, X. Xing, and X.-C. Wu. 2013. Turtles from the Jurassic Shishugou Formation of the Junggar Basin, People's Republic of China, and the basicranial region of basal eucryptodires; pp. 147–172 in D. B. Brinkman, J. D. Gardner, and P. A. Holroyd (eds.), Morphology and Evolution of Turtles. Springer, Dordrecht.

Chkhikvadze, V. M. 1975. [Volume and systematic position of turtles of the suborder Amphichelydia Lydekker, 1899]. Soobscheniya AN Gruzinskoy SSRR 78:745–748. [Russian]

Chkhikvadze, V. M. 1977. [Fossil turtles of the family Sinemydidae. Izvestiya AN Gruzinskoy SSR]. Seriya Biologicheskaya 3:265–270. [Russian]

Chkhikvadze [Čkhikvadze], V. M. 1987. Sur la classification et les charactéres de certaines tortues fossiles d'Asie, rares et peu etudiees. Studia Geologica Salmaticensia, Studia Palaeocheloniologica 2:55–85.

Danilov, I. G., and J. F. Parham. 2006. A redescription of '*Plesiochelys tatsuensis*' from the Late Jurassic of China, with comments on the antiquity of the crown clade Cryptodira. Journal of Vertebrate Paleontology 26:573–580.

Danilov, I. G., and J. F. Parham. 2007. The type series of '*Sinemys*' *wuerhoensis*, a problematic turtle from the Lower Cretaceous of China, includes at least three taxa. Palaeontology 50:431–444.

Danilov, I. G., and J. F. Parham. 2008. A reassessment of some poorly known turtles from the Middle Jurassic of China, with comments on the antiquity of extant turtles. Journal of Vertebrate Paleontology 28:306–318.

Endo, R., and T. Shikama. 1942. Mesozoic reptilian fauna in the Jehol mountainland, Manchoukuo. Bulletin of Central National Museum of Manchoukuo 3:1–19.

Fang, Q.-R. 1987. A new species of Middle Jurassic turtle from Sichuan. Acta Herpetologica Sinica 6:65–9.

Gaffney, E. S. 1972. An illustrated glossary of turtle skull nomenclature. Amercian Museum Novitates 2486:1–33.

Gaffney, E. S. 1979. Comparative cranial morphology of Recent and fossil turtles. Bulletin of the American Museum of Natural History 164:69–376.

Gaffney, E. S. 1996. The postcranial morphology of *Meiolania platyceps* and a review of the Meiolaniidae. Bulletin of the American Museum of Natural History 229:1–166.

Gaffney, E. S., and X. Ye. 1992. *Dracochelys*, a new cryptodiran turtle from the Early Cretaceous of China. American Museum Novitates 3048:1–13.

Gaffney, E. S., J. H. Hutchison, F. A. Jenkins, and L. J. Meeker. 1987. Modern turtle origins: the oldest known cryptodire. Science 237:289–291.

Gaffney, E. S., L. Kool, D. B. Brinkman, T. H. Rich, and P. Vickers-Rich. 1998. *Otwayemys*, a new cryptodiran turtle from the Early Cretaceous of Australia. American Museum Novitates 3233:1–28.

Gaffney, E. S., T. H. Rich, P. Vickers-Rich, A. Constantine, R. Vacca, and L. Kool. 2007. *Chubutemys*, a new eucryptodiran turtle from the Early Cretaceous of Argentina, and the relationships of Meiolaniidae. American Museum Novitates 3599:1–35.

Goloboff, P. A., C. I. Mattoni, and A. S. Quinteros. 2008. TNT, a free program for phylogenetic analysis. Cladistics 24:774–786.

Gubin, Y. M., and S. M. Sinitza. 1996. Shar Teg: a unique Mesozoic locality of Asia. Museum of Northern Arizona Bulletin 60:311–318.

Herrel, A. J., C. O'Reilly, and A. M. Richmond. 2002. Evolution of bite performance in turtles. Journal of Evolutionary Biology 15:1083–1094.

Hirayama, R., D. B. Brinkman, and I. G. Danilov. 2000. Distribution and biogeography of non-marine Cretaceous turtles. Russian Journal of Herpetology 7:181–198.

Hutchison, J. H., and J. D. Archibald. 1986. Diversity of turtles across the Cretaceous/Tertiary Boundary in northeastern Montana. Palaeogeography, Palaeoclimatology, Palaeoecology 55:1–22.

Hutchison, J. H., and D. M. Bramble. 1981. Homology of the plastral sclaes of the Kinosternidae and related turtles. Herpetologica 37(2):73–85.

International Commission on Zoological Nomenclature. 1999. International Code of Zoological Nomenclature, Fourth Edition. International Trust for Zoological Nomenclature, London, 306 pp.

Joyce, W. G. 2007. Phylogenetic relationships of Mesozoic turtles. Bulletin of the Peabody Museum of Natural History 48:3–102.

Joyce, W. G., and C. J. Bell. 2004. A review of the comparative morphology of extant testudinoid turtles (Reptilia: Testudines). Asiatic Herpetological Research 10:53–109.

Joyce, W. G., and J. Sterli. 2012. Congruence, non-homology, and the phylogeny of basal turtles. Acta Zoologica 93:149–159.

Joyce, W. G., F. A. Jenkins, and T. Rowe. 2006. The presence of cleithra in the primitive turtle *Kayentachelys aprix*. Russian Journal of Herpetology 13, Supplement (Fossil Turtle Research 1):93–103.

Joyce, W. G., J. F. Parham, and J. A. Gauthier. 2004. Developing a protocol for the conversion of rank-based taxon names to phylogenetically defined clade names, as exemplified by turtles. Journal of Paleontology 78:989–1013.

Joyce, W. G., J. F. Parham, T. R. Lyson, R. C. M. Warnock, and P. C. J. Donoghue. 2013. A divergence dating analysis of turtles using fossil calibrations: an example of best practices. Journal of Paleontology 87:612–634.

Kaznyshkin, M. N., L. A. Nalbandyan, and L. A. Nessov. 1990. [Middle and Late Jurassic turtles of Fergana (Kirghiz SSR)]. Yezhegodnik Vsesoyuznogo Paleontologicheskogo Obshchestva [Annual of the All-union Palaeontological Society]] 33:185–204. [Russian]

Khosatzky L. I., and L. A. Nessov. 1979. [Large turtles of the Late Cretaceous of Middle Asia]. Trudy Zoologicheskogo Instituta AN SSSR 89:98–108. [Russian].

Klein, I. T. 1760. Klassification und kurze Geschichte der Vierfüßigen Thiere (translation by F. D. Behn). Jonas Schmidt, Lübeck, 381 pp.

Krenz, J. G., G. J. P. Naylor, H. B. Shaffer, and F. J. Janzen. 2005. Molecular phylogenetics and evolution of turtles. Molecular Phylogenetics and Evolution 37:178–191.

Maisch, M. A., A. Matzke, and G. Sun. 2003. A new sinemydid turtle (Reptilia: Testudines) from the Lower Cretaceous of the Junggar Basin (NW-China). Neues Jahrbuch für Geologie und Paläontologie, Monatshefte 2003(12):705–722.

Matzke, A. T., M. W. Maisch, H.-U. Pfretzschner, G. Sun, and H. Stöhr. 2004a. A new basal sinemydid turtle (Reptilia: Testudines) from the Lower Cretaceous Tugulu Group of the Junggar Basin (NW China). Neues Jahrbuch für Geologie und Paläontologie, Monatshefte 2004(3):151–167.

Matzke, A. T., M. W. Maisch, G. Sun, H.-U. Pfretzschner, and H. Stöhr. 2004b. A new xinjiangchelyid turtle (Testudines, Eucryptodira) from the Jurassic Qigu Formation of the southern Jungar Basin, Xinjiang, North-West China. Palaeontology 47:1267–1299.

Matzke, A. T., M. W. Maisch, G. Sun, H.-U. Pfretzschner, and H. Stöhr. 2005. A new Middle Jurassic xinjiangchelyid turtle (Testudines; Eucryptodira) from China (Xinjiang, Junggar Basin). Journal of Vertebrate Paleontology 25:63–70.

Nessov, L. A. 1995. On some Mesozoic turtles of the Fergana Depression (Kyrgyzstan) and Dzhungar Alatau Ridge (Kazakhstan). Russian Journal of Herpetology 2:134–141.

Nessov, L. A., and L. I. Khosatzky. 1973. [Early Cretaceous turtles from southeastern Fergana]; pp. 132–133 in Problems in Herpetology: Proceedings of the 3rd All-union Herpetological Conference, Leningrad, 1–3 February 1973. Zoological Institute of the Academy of Sciences USSR, Leningrad. [Russian]

Nessov, L. A., and L. I. Khosatzky. 1981. [Turtles of the Early Cretaceous of Transbaikalia]; pp. 74–78 in L. J. Borkin (ed.), [Herpetological Investigations in Siberia and the Far East]. Academy of Sciences of the USSR, Leningrad. [Russian]

Parham, J. F., and J. H. Hutchison. 2003. A new eucryptodiran turtle from the Late Cretaceous of North America (Dinosaur Provincial Park, Alberta, Canada). Journal of Vertebrate Paleontology 23:783–798.

Peng, G., Y. Ye, Y. Gao, C. Shu, and S. Jiang. 2005. Jurassic Dinosaur Faunas in Zigong. Zigong Dinosaur Museum, Zigong, 236 pp. [Chinese with English translation]

Peng, J.-H., and D. B. Brinkman. 1993. New material of *Xinjiangchelys* (Reptilia: Testudines) from the Late Jurassic Qigu Formation (Shishugou Group) of the Pingfengshan locality, Junggar Basin, Xinjiang. Canadian Journal of Earth Sciences 30:2013–2026.
Rabi, M., W. G. Joyce, and O. Wings. 2010. A review of the Mesozoic turtles of the Junggar Basin (Xinjiang, Northwest China) and the paleobiogeography of Jurassic to Early Cretaceous Asian Testudinates. Paleobiodiversity and Paleoenvironments 90:259–273.
Ryabinin, A. N. 1948. [Turtles from the Jurassic of Kara-Tau]. Trudy Paleontologiicheskogo Instituta AN SSSR 15:94–98. [Russian]
Schumacher, G. H. 1973. The head muscles and hyolaryngeal skeleton of turtles and crocodilians; pp. 101–199 in C. Gans and T. Parsons (eds.), Biology of the Reptilia, Volume 4. Academic Press, London and New York.
Sinitshenkova, N. D. 1995. New Late Mesozoic stoneflies from Shar Teg, Mongolia (Insecta: Perlida = Plecoptera). Paleontological Journal 29:93–104.
Sinitshenkova, N. D. 2002. New Late Mesozoic mayflies from the Shar Teg locality, Mongolia (Insecta, Ephemerida = Ephemeroptera). Paleontological Journal 36:43–48.
Sterli, J. 2008. A new, nearly complete stem turtle from the Jurassic of South America with implications for turtle evolution. Biology Letters 4:286–289.
Sterli, J. 2010. Phylogenetic relationships among extinct and extant turtles: the position of Pleurodira and the effects of the fossils on rooting crown-group turtles. Contributions to Zoology 79(3):93–106.
Sterli, J., and M. de la Fuente. 2010. Anatomy of *Condorchelys antiqua* Sterli, 2008, and the origin of the modern jaw closure mechanism in turtles. Journal of Vertebrate Paleontology 30:351–366.
Sterli, J., and M. de la Fuente. 2011. A new turtle from the La Colonia Formation (Campanian–Maastrichtian), Patagonia, Argentina, with remarks on the evolution of the vertebral column in turtles. Palaeontology 54:63–78.
Sterli, J., and M. de la Fuente. 2013. New evidence from the Palaeocene of Patagonia (Argentina) on the evolution and palaeobiogeography of meiolaniid-like turtles (Testudinata). Journal of Systematic Palaeontology 11:835–852.
Sterli, J., D. Pol., and M. Laurin. 2013. Incorporating phylogenetic uncertainty on phylogeny-based palaeontological dating and the timing of turtle diversification. Cladistics 29:233–246.
Sukhanov [Suhanov], V. B. 1964. Subclass Testudinata, Testudinates; pp. 354–438 in A. K. Rožděstvenskij and L. P. Tatarinov (eds.), [Fundamentals of Paleontology; Amphibians, Reptiles and Birds]. Nauka, Moscow. [Russian]
Sukhanov, V. B. 2000. Mesozoic turtles of Middle and Central Asia; pp. 309–367 in M. J. Benton, M. A. Shishkin, D. M. Unwin, and E. N. Kurochkin (eds.), The Age of Dinosaurs in Russia and Mongolia. Cambridge University Press, Cambridge, U.K.
Sukhanov, V. B., and P. Narmandakh. 1974. [New Early Cretaceous turtle from the continental deposits of the Northern Gobi]; pp. 192–220 in Mesozoic and Cenozoic Faunas and Bistratigraphy of Mongolia. The Joint Soviet-Mongolian Paleontological Expedition, Transactions, 1. Nauka Publishers, Moscow. [Russian]
Sukhanov, V. B., and P. Narmandakh. 2006. New taxa of Mesozoic turtles from Mongolia. Fossil Turtle Research 1:119–127.
Tatarinov, L. P. 1959. [A new turtle of the family Baenidae from the Lower Eocene of Mongolia]. Paleontologicheskiy Zhurnal 1:100–113. [Russian]
Tong, H., and D. Brinkman. 2013. A new species of *Sinemys* (Testudines: Cryptodira: Sinemydidae) from the Early Cretaceous of Inner Mongolia, China. Palaeobiodiversity and Palaeoenvironments 93:355–366.
Tong, H., E. Buffetaut, and V. Suteethorn. 2002. Middle Jurassic turtles from southern Thailand. Geological Magazine, 139:687–697.
Tong, H., S.-A. Ji, and Q. Ji. 2004. *Ordosemys* (Testudines: Cryptodira) from the Yixian Formation of Liaoning Province, northeastern China: new specimens and systematic revision. American Museum Novitates 3438:1–20.
Tong, H., I. G. Danilov, Y. Ye, H. Ouyang, and G. Peng. 2012a. Middle Jurassic turtles from Sichuan Basin, China: a review. Geological Magazine 149:675–695.
Tong, H., I. G. Danilov, Y. Ye, H. Ouyang, G. Peng, and K. Li. 2012b. A revision of xinjiangchelyid turtles from the Late Jurassic of Sichuan Basin, China. Annales de Paléontologie 98:73–114.
Tong, H., J. Claude, W. Naksri, V. Suteethorn, E. Buffetaut, S. Khansubha, K. Wongko, and P. Yuangdetkla. 2009. *Basilochelys macrobios* n. gen. and n. sp., a large cryptodiran turtle from the Phu Kradung Formation (latest Jurassic–earliest Cretaceous) of the Khorat Plateau, NE Thailand. Geological Society of London Special Publications 315:153–173.
Watabe, M., K. Tsogtbaatar, L. Uranbileg, and L. Gereltsetseg. 2004. Report on the Japan-Mongolia Joint Paleontological Expedition to the Gobi desert, 2002. Hayashibara Museum of Natural Sciences Research Bulletin 2:97–122.
Wiman, C. 1930. Fossile Schildkröten aus China. Paleontologia Sinica, Series C 6:1–56.
Wings, O., M. Rabi, J. W. Schneider, L. Schwermann, G. Sun, C.-F. Zhou, and W. G. Joyce. 2012. An enormous Jurassic turtle bone bed from the Turpan basin of Xinjiang, China. Naturwissenschaften 99:925–935.
Ye, X. 1963. Fossil turtles of China. Palaeontologica Sinica, Series C 150:1–113.
Ye, X. 1982. Middle Jurassic turtles from Sichuan, SW China. Vertebrata PalAsiatica 20:282–290.
Ye, X. 1986. A Jurassic turtle from Junggar, Xinjiang. Vertebrata PalAsiatica 24:171–181.
Ye, Y. 1999. A new genus of Sinemydidae from the Late Jurassic of Neijiang, Sichuan. Vertebrata PalAsiatica 37:81–87.
Young, C.-C., and M.-C. Chow. 1953. New fossil reptiles from Szechuan, China. Acta Scientia Sinica 2:216–229.
Zhou, C.-F. 2010a. A new eucryptodiran turtle from the Early Cretaceous Jiufotang Formation of western Liaoning, China. Zootaxa 2676:45–56.
Zhou, C.-F. 2010b. A second specimen of *Manchurochelys manchoukuoensis* Endo & Shikama, 1942 (Testudines: Eucryptodira) from the Early Cretaceous Yixian Formation of western Liaoning, China. Zootaxa 2534:57–66.

Submitted January 7, 2013; revisions received May 4, 2013; accepted May 16, 2013.
Handling editor: Juliana Sterli.

APPENDIX 1. List of taxa omitted from the matrix of Sterli and de la Fuente (2013).

Ninjemys oweni, Warkalania carinaminor, Patagoniaemys gasparinae, Otwayemys cunicularius, Prochelidella cerrobarcinae, Mychelys latisternum, Chelodina colliei, Yaminuchelys maior, Dinochelys whitei, Neurankylus eximius, Boremys pulchra, Baena arenosa, Chisternon undatum, Macroclemys schmidti, Protochelydra zangerli, Chelonidis gringorum, Stylemys nebraskensis, Echmatemys wyomingensis, Xenochelys formosa, Hoplochelys crassa, Plastomenus aff. thomassii, and *Anosteira ornata.*

APPENDIX 2. List of taxa designated as floaters after constraining the relationships of Durocryptodira in the phylogenetic analysis.

Siamochelys peninsularis, Basilochelys macrobios, Ordosemys leios, Dracochelys bicuspis, Judithemys sukhanovi, Hangaiemys hoburensis, Xinjiangchelys junggarensis, Xinjiangchelys radiplicatoides, Annemys latiens, Annemys levensis, Shachemys laosiana, Adocus beatus, Yehguia tatsuensis, Basilemys variolosa, Baptemys wyomingensis, all members of Trionychidae and Panpleurodira*, Toxochelys latiremis, Mesodermochelys undulatus, Plesiochelys etalloni, Santanachelys gaffneyi, Solnhofia parsonsi,* and *Portlandemys mcdowelli.*

NOTE ADDED AT PROOF

While this paper was in print, a modified version of the taxon-character matrix developed herein was published by the senior author and co-authors. The reference for this paper is:

Rabi, M., Zhou, C.-F., Wings, O., Sun, G., Joyce, W. G. 2013. A new xinjiangchelyid turtle from the Middle Jurassic of Xinjiang, China and the evolution of the basipterygoid process in Mesozoic Turtles. BMC Evolutionary Biology 13:203.